mRNA localisation, reaction centre biogenesis and thylakoid membrane targeting in cyanobacteria

Moontaha Mahbub[1,2], Luisa Hemm[3], Yuxiao Yang[1], Ramanpreet Kaur[1], Helder Carmen[1], Christoph Engl[1], Tuomas Huokko[4], Matthias Riediger[3], Satoru Watanabe[5], Lu-Ning Liu[4,6], Annegret Wilde[3], Wolfgang R. Hess[3] and Conrad W. Mullineaux[1*]

[1]School of Biological and Chemical Sciences, Queen Mary University of London, London, U.K.

[2]Department of Botany, Jagannath University, Dhaka 1100, Bangladesh

[3]Institute of Biology III, University of Freiburg, Freiburg, Germany

[4]Institute of Integrative Biology, University of Liverpool, Liverpool, U.K.

[5]Department of Bioscience, Tokyo University of Agriculture, Tokyo, Japan

[6]College of Marine Life Sciences, and Frontiers Science Center for Deep Ocean Multispheres and Earth System, Ocean University of China, Qingdao 266003, China

*e-mail: c.mullineaux@qmul.ac.uk

Abstract

The thylakoid membranes of cyanobacteria form a complex intracellular membrane system with a distinctive proteome. The sites of biogenesis of thylakoid proteins remain uncertain, as do the signals that direct thylakoid membrane-integral proteins to the thylakoids rather than to the plasma membrane. Here, we address these questions by using Fluorescent *in situ* Hybridisation to probe the subcellular location of mRNA molecules encoding core subunits of the photosystems in two cyanobacterial species. These mRNAs cluster at thylakoid surfaces mainly adjacent to the central cytoplasm and the nucleoid, in contrast to mRNAs encoding proteins with other locations. Ribosome association influences the distribution of the photosynthetic mRNAs on the thylakoid surface, but thylakoid affinity is retained in the absence of ribosome association. However, thylakoid association is disrupted in a mutant lacking two mRNA-binding proteins, which likely play roles in targeting photosynthetic proteins to the thylakoid membrane.

Cyanobacterial thylakoid membranes form a complex intracellular membrane system that has been inherited, with modifications, in chloroplasts. Cyanobacterial thylakoids are the sole site of photosynthetic electron transport and the major site of respiration, and they have a proteome distinct from that of the plasma membrane[1–3]. Membrane architecture varies between species, but the thylakoids usually form a series of flattened sacs located between the plasma membrane and the central cytoplasm[4–8]. Electron tomography indicates that the thylakoids and the plasma membrane are not contiguous[5,7], although in some cyanobacteria, such as *Synechocystis* sp. PCC 6803 (hereafter *Synechocystis*), the sacs converge on a membrane tube which closely approaches the plasma membrane at some sites[7].

Thylakoid membranes have a distinctive proteome that includes all the complexes involved in photosynthetic electron transport, and most of the respiratory complexes[1,3], organised in a dynamic and variable protein landscape[9]. An early study suggested that the initial steps of photosystem biogenesis occurred in the plasma membrane[10], but an improved cell fractionation procedure showed that Photosystem II (PSII) biogenesis takes place in the thylakoids[11]. Biochemical and mutagenesis studies have revealed an intricate, co-ordinated sequence of events by which the photosynthetic reaction centre apoproteins, along with their chlorophylls and other co-factors, are synthesised and assembled into mature reaction centres[1,12–14], but the exact locations of these processes remain uncertain. In *Synechocystis*, a specialised biogenic region was proposed at the convergence membrane adjacent to the plasma membrane. PratA, a periplasmic protein implicated in the delivery of manganese ions to the water-oxidising complex of PSII, is concentrated near the convergence zones, suggesting that these are a major site of PSII biogenesis[12,15,16]. Cryo-electron tomography shows some ribosomes associated with the convergence membranes, although the vast majority of thylakoid-associated ribosomes are found at the innermost thylakoid surface, facing the central cytoplasm[7]. An earlier electron tomographic study highlighted a high density of ribosomes associated with protrusions of the thylakoid system into the central cytoplasm[6].

Mechanisms for specific targeting of proteins to the thylakoid or plasma membrane remain uncertain. Membrane-targeted proteins commonly carry N-terminal leader sequences that should be specific for the Sec or Tat translocons[17]. However, *Synechocystis* has only a single set of genes for each translocon, and it is likely that the same sets of Sec and Tat components are present in both thylakoid and plasma membranes[17]. Intensive studies of the

leader sequences have not revealed any differences that could lead to predictable targeting to a specific membrane[17]. It was accordingly suggested that protein sorting might occur post-translationally, based on differences in the electrostatic properties of the C-terminal portions of the polypeptides[1]. This would require connections (at least transiently) between the thylakoid and plasma membranes, to allow sorting by lateral diffusion after translation. Such connections are rarely observed[7].

Here, we use Fluorescent *in situ* Hybridisation (FISH) to probe the subcellular location of mRNA molecules encoding core subunits of the photosystems in two species of cyanobacteria. The results give clues to the sub-cellular location of the first stage of photosystem assembly, and the mechanism that targets photosynthetic proteins to the thylakoids.

Rationale for RNA-FISH experiments

To better understand the targeting and biogenesis of cyanobacterial thylakoid membrane proteins, we probed the subcellular location of specific mRNAs encoding photosynthetic proteins. The expectation is that cyanobacterial membrane-integral proteins should be inserted co-translationally via the Signal Recognition Particle (SRP)-dependent pathway[17,18]. Essentially all *psbA* mRNA in *Synechocystis* and in *Synechococcus elongatus* PCC 7942 (hereafter *Synechococcus*) is ribosome-associated: translational control is achieved through pausing at distinct sites[19,20]. Therefore, the location of the mRNA should reveal the site of membrane integration of the protein. We used a single-molecule RNA-FISH protocol which uses a set of 40-48 short single-stranded DNA probes, each about 20 bases long and with a fluorophore attached to the 3' end[21]. The high sensitivity and specificity of the technique come from the large number of fluorophores that can be associated with each mRNA molecule, and the need for multiple probes to hybridise in the same place to produce a fluorescent focus[21].

We selected two unicellular cyanobacterial model species. S*ynechocystis* is the most widely-used cyanobacterial model for photosynthesis research, and its membrane architecture has been intensively studied[6,7]. Except where otherwise stated, we used the PCC-M variant[22], which has larger cells than some of the sub-strains. *Synechococcus* has a different cell architecture, with rod-shaped cells and thylakoid membranes that lack obvious convergence zones or central extensions[23,24]. The thylakoids approximate to a set of nested concentric cylinders aligned along the

long axis of the cell, and their regular conformation is conducive to quantitative microscopy[23,25,26]. Both organisms have chlorophyll *a* and phycocyanin as their major photosynthetic pigments. We therefore employed oligonucleotide probes linked to TAMRA (5-Carboxytetramethylrhodamine) whose absorption and emission maxima (respectively 552 nm and 576 nm) are distinct from the photosynthetic pigments.

Practical aspects of RNA-FISH in cyanobacteria

RNA-FISH experiments require cell fixation followed by permeabilisation with 70% ethanol before probing[21]. This treatment removes much of the chlorophyll, but the phycobilins are retained. Phycobilin fluorescence allows visualisation of the thylakoids in the treated cells, and cell structure as probed by confocal fluorescence microscopy shows little difference from live cells (Extended Data Fig. 1a-e). The fixed cells retained high background fluorescence across the spectrum, mostly originating from the thylakoids (Extended Data Fig. 1f,g). Therefore, we could only detect reliable FISH signals from abundant mRNA species, and imaging required extreme care since exposure to the excitation light easily photobleached the FISH signal whilst enhancing the background fluorescence. This issue precluded repeated imaging to obtain *z*-stacks or to image multiple probes simultaneously. FISH imaging in cyanobacteria proved less straightforward than in e.g. *Escherichia coli*, where background fluorescence is low compared to the FISH signal[21]. However, we found that the problems in cyanobacteria could be mitigated because the background signal in the TAMRA channel is reliably predictable from the thylakoid image in the red channel. This allows subtraction of the background from images of probed cells to give a cleaner image of mRNA location (Extended Data Fig. 2).

Probing for *psbA* mRNA

We first probed for the highly expressed *psbA* mRNAs encoding the D1 subunit of PSII (Fig. 1,2). We designed probes against the most highly expressed *psbA* genes (*psbA2* in *Synechocystis*[27] and *psbA1* in *Synechococcus*[28]), but, in both species, the strong nucleotide sequence conservation within the *psbA* gene families means that the FISH probes (Supplementary Table 1) must recognise a mixture of *psbA* mRNAs. A *Synechocystis psbA2* null mutant still showed a *psbA* FISH signal (likely from *psbA3* mRNA[27]), albeit at reduced intensity (Extended Data Fig. 3). We checked for specificity of the probes for the *psbA* species using a *Synechocystis* triple knockout mutant lacking all three *psbA* genes[29]. Unlike the wild type (Extended Data Fig. 1-3), this mutant shows occasional concentrations of fluorescence

in the TAMRA channel even in unprobed cells, likely reflecting accumulation of pigment precursors or breakdown products due to perturbed reaction centre biogenesis However, the signal was not significantly different in probed vs unprobed cells (Extended Data Fig. 3).

psbA FISH signals were decreased, although not completely abolished, by treatment with the RNA polymerase inhibitor rifampicin for 1 hour (Extended Data Fig. 4). The residual signal likely reflects slow degradation of some mRNA following rifampicin treatment. *psbA* mRNAs have relatively long half-lives in *Synechococcus* (18-25 min for *psbA1*)[28]. The FISH signal increased in high light-treated cells, where *psbA* expression is expected to increase[27,28] (Fig. 2a,b). In some cells, the *psbA* FISH signals were clearly distinct from the location of the nucleoid, as probed with 4',6-diamidino-2-phenylindole (DAPI) staining (Extended Data Fig. 5). This suggests that the FISH probe does not hybridise with DNA sequences, as expected since the RNA-FISH protocol does not include a denaturation step to separate double-stranded DNA[21].

Location of *psbA* mRNA

Cells probed with the *psbA* probe-sets showed concentrations of TAMRA fluorescence with distributions distinct from the background (Fig. 1,2). Given the low overlap between TAMRA emission and cell absorption, and the generally low level of light absorption at the single-cell level[30], distortion of the patterns by fluorescence re-absorption is not a significant concern. In *Synechocystis*, *psbA* FISH signals were concentrated at the inner surface of the thylakoid system and around protrusions of the thylakoid system into the central cytoplasm (Fig. 1a). TAMRA fluorescence in the central cytoplasm was almost invariably associated with such protrusions, which were identifiable by fluorescence in the red channel from photosynthetic pigments. Fig. 1a shows representative examples of these fluorescence distributions as observed by confocal microscopy, with line profiles to demonstrate the close coincidence between concentrations of TAMRA fluorescence and thylakoid membrane signals.

To investigate the relationship between *psbA* mRNA and thylakoid membrane structures at higher spatial resolution, we used fluorescence microscopy with super-resolution radial fluctuations (SRRF)-Stream technology[31] (Fig. 1b). These images have higher spatial resolution than the confocal images, but lower spectral resolution (see Methods), and we were not able to use background subtraction to remove the background autofluorescence as with the

confocal images. Therefore, these images show background autofluorescence in addition to the RNA-FISH signal. However, the SRRF images confirm the presence in many cells of very fine thylakoid membrane protrusions into the central cytoplasm, and suggest that these protrusions are frequently associated with concentrations of *psbA* mRNA (Fig. 1b). We did not observe similar thylakoid protrusions in the thinner and rod-shaped *Synechococcus* cells, where all the photosynthetic pigment fluorescence comes from regular tubes of thylakoid membrane layers surrounding the thinner central cytoplasm (Fig. 2). In *Synechococcus* cells grown under our standard conditions, *psbA* FISH signals were concentrated in localised patches at the thylakoids (Fig. 2 a,d). The regular conformation of the cells and the thylakoids in *Synechococcus* enables quantitation of distributions and merging data from multiple cells. Fig. 2d shows line profiles drawn along the long and short axes, merged from 50 cells. The merged long-axis profile reveals a high frequency of *psbA* mRNA spots towards the inner edge of the thylakoid system near the poles of the cell, although spots can also be found in other locations (Fig. 2d). The merged short-axis profile shows that *psbA* mRNA is concentrated near the inner edge of the thylakoid system, with a distinct dip in signal in the central cytoplasm and no detectable signal at the outer edge of the thylakoids adjacent to the plasma membrane (Fig. 2d). *Synechocystis* cells also show very little *psbA* FISH signal adjacent to the plasma membrane: the signal is overwhelmingly concentrated at the inner surfaces of the thylakoid system (Fig. 1).

psbA mRNA in PSII biogenesis vs. repair

Cyanobacterial *psbA* expression is often connected with PSII repair after photodamage, rather than *de novo* biogenesis[13]. To get a clearer picture of mRNA location associated with the two processes, we took advantage of the regular conformation of *Synechococcus* cells to quantify *psbA* mRNA distribution under different conditions. We induced photodamage by exposure of low light-grown cells to high light (HL) for 1 h. Such treatments are known to induce high levels of *psbA* mRNA[28], and as expected, we found that HL-treatment caused a strong increase in the mean cellular *psbA* signal (Fig. 2b), although expression levels differ markedly in different individual cells (Fig. 2a,b). Although the *psbA* FISH signal in HL cells was still clearly thylakoid-associated, it appeared more evenly distributed along the thylakoid surface than in low light cells. To quantify this effect, we used a method previously used to quantify the patchiness in the distribution of a GFP-tagged thylakoid protein[25]: this involves tracing a line around the thylakoids in each cell image and plotting fluorescence as a function of distance along the line. Evenly-distributed fluorescence fluctuates little along the line profile and therefore has a low standard deviation, whereas patchy

fluorescence has a high standard deviation[25]. The standard deviation (normalised to the total fluorescence) therefore provides a quantitative measure of the patchiness of the signal. This analysis demonstrates that HL treatment makes the *psbA* FISH signal significantly less patchy (Fig. 2c).

Influence of ribosomes on *psbA* mRNA location

To explore the role of ribosomes in determining *psbA* mRNA localisation, we carried out FISH measurements on cells preincubated with lincomycin, which blocks translation elongation[20], and puromycin, which blocks translation elongation and additionally releases the mRNA from the ribosome[32]. We confirmed that inhibitor treatments did not increase the background fluorescence in unprobed cells, and that puromycin at 50 μg ml^{-1} was sufficient to kill all cells in the culture (Extended Data Fig. 6). In our FISH experiments we used puromycin at 500 μg ml^{-1}. Both inhibitors induced substantial increases in FISH signal in a subset of the cells (Fig. 1a,c; Fig. 2 d,e). Blocking translation has previously been shown to increase the stability of *psbA* transcripts[33,34], and Northern blot analysis confirmed that the inhibitor treatments increase *psbA2* transcript levels in *Synechocystis* (Extended Data Fig. 7). Both ribosome inhibitors significantly changed the mRNA distribution, which became less patchy in the treated cells (Fig. 1a,d; Fig 2d,f). In puromycin-treated *Synechocystis, psbA* mRNA often appeared to coat the inner edge of the thylakoid system, whereas lincomycin treatment led to accumulation of the transcript in the central cytoplasm away from the thylakoids (Fig. 1a). Similar effects were quantifiable in *Synechococcus* (Fig. 2 d,g,h) where both inhibitors caused a significant increase in the mean distance between the *psbA* FISH signals and the thylakoids (Fig. 2h). However, the effect of lincomycin was greater (Fig. 2h), and, in lincomycin-treated cells, the short axis line-profiles suggest very little thylakoid association (Fig. 2g). By contrast, *psbA* mRNA in puromycin-treated cells retains a distinct bias in its distribution towards the thylakoids (Fig. 2g). The significant effects of the inhibitors indicate that *psbA* mRNA location is influenced by association with ribosomes, consistent with previous findings that *psbA* mRNA is all ribosome-associated in cyanobacteria[19]. Nevertheless, a clear association of *psbA* mRNA with the thylakoid inner surface and protrusions was retained after treatment with a high concentration of puromycin (Fig. 1a; Fig 2d,g,h).

Location of *psaA* mRNA

To probe the location of Photosystem I (PSI) biogenesis, we carried out similar FISH experiments with probes hybridising to the *psaA* part of the *psaAB* transcript encoding the PSI core subunits (Fig. 3; Extended Data Figs 8,9).

The *psaA* FISH signals show sharply punctate distributions. As with *psbA* (Figs 1,2), there are concentrations in discrete patches at the thylakoid inner surface in *Synechococcus* (Fig. 3b), and around the thylakoid extensions in *Synechocystis* (Fig. 3a). In contrast to their effects on *psbA* transcript levels (Fig. 1,2; Extended Data Fig. 7), both puromycin and lincomycin strongly decreased the *psaA* FISH signal, suggesting destabilisation of the *psaAB* mRNA (Fig. 3). Northern blot analysis confirmed this effect (Extended Data Fig. 7). Inhibited cells showed residual FISH signals in patches at the thylakoid inner surfaces (Fig. 3). Although the low residual signal precluded plotting of distance distributions as for *psbA* (Fig. 2h), results are consistent with a thylakoid affinity that does not depend on active translation or ribosome association.

Location of other mRNAs

To test whether location at the inner surface of the TM was specific to mRNAs encoding membrane-integral thylakoid components, we probed the locations of two abundant mRNA species encoding proteins with other locations: *cpcAB* in *Synechocystis* and *rbcL* in *Synechococcus* (Fig. 4). *cpcAB* encodes the α- and β-subunits of phycocyanin, the major protein component of the phycobilisome light-harvesting complexes. These proteins are water-soluble and associated with the cytoplasmic surface of the thylakoid membrane[35]. *rbcL* encodes the large subunit of ribulose-1,5-bisphosphate carboxylase, a cytoplasmic enzyme that is mainly packaged into carboxysomes: icosahedral organelles with a protein shell that are located in the central cytoplasm[36–39]. *cpcAB* mRNA showed a patchy distribution mainly in the central cytoplasm of *Synechocystis* (Fig. 4a). Comparison of *cpcAB* distribution with *psbA* and *psaA* confirms closer association of both *psbA* and *psaA* mRNAs with the membrane in *Synechocystis* (Fig. 4b). *psbA* and *psaA* mRNAs showed similar distance distributions, but *cpcAB* mRNA was significantly further from the thylakoids (Fig. 4b). We probed *rbcL* mRNA in a *Synechococcus* mutant expressing GFP-tagged RbcL[39,40]. The GFP signal is concentrated in semi-regularly spaced spots in the central cytoplasm which clearly correspond to the carboxysomes[36] (Fig. 4c). The *rbcL* FISH signal is also found in spots in the central cytoplasm (Fig. 4c). These spots sometimes coincide with the carboxysomes, but they are much less numerous (Fig. 4c). It is possible that *rbcL* mRNA co-localises with a sub-population of nascent carboxysomes, but this point needs further investigation. Short-axis line profiles show that the distribution of *rbcL* mRNA is centred in the middle of the central cytoplasm, similarly to the RbcL-GFP signal (Fig. 4d) and in contrast to *psbA* (Fig. 2g). The distances of spots of *rbcL* mRNA from the nearest

thylakoid (Fig. 4e) show a different distribution from *psbA* and *psaA* (Fig 3e). *psbA* and *psaA* mRNAs are quantifiably closer to the thylakoids than *rbcL* ($p = 10^{-6}$ for *psbA* and 10^{-5} for *psaA*).

Involvement of mRNA-binding proteins

Results in Figs 1-4 suggest that proximity to thylakoid surfaces may be specific to mRNAs encoding membrane-integral thylakoid proteins, and that thylakoid affinity of these mRNAs can be independent of ribosome association. This raises the possibility of RNA-binding proteins (RBPs) that might bind specifically to this set of mRNAs and help to anchor them at the thylakoid membrane. Accordingly, we investigated two putative *Synechocystis* RBPs: Rbp2 (ssr1480) and Rbp3 (slr0193). Mutants were constructed in the glucose-tolerant *Synechocystis* GT-I background[41] in which each of these proteins was FLAG-tagged, and pull-downs of the FLAG-tagged protein were probed for *psbA2* and *psaA* mRNAs. Rbp2 bound *psbA2* mRNA (Fig. 5a) and Rbp3 bound both *psbA2* and *psaA* mRNA, including an untranslated upstream region resulting from a second transcriptional start-site (Fig. 5b). Biochemical fractionation showed that Rbp3 is strongly membrane-associated (Extended Data Fig. 10). We then investigated a mutant lacking Rbp2 and Rbp3 (GT-I::Δ*rbp2/3*). This mutant showed some growth perturbation, with a prolonged lag phase after transfer to higher light intensity and slightly slower growth than wild type in the presence of glucose (Extended Data Fig. 10). It had perturbed pigment content, with lower pigment per cell and a lower content of PSI relative to PSII (Extended Data Fig. 10). FISH measurements showed perturbed location of both *psbA* and *psaA* mRNAs in GT-I::Δ*rbp2/3*, with concentrations in the central cytoplasm that appeared detached from the thylakoids (Fig. 5c,f). Analysis of the distance between the mRNA concentration and the nearest thylakoid confirmed that the location of both mRNAs was significantly perturbed, but with a stronger effect on *psaA* (Fig. 5i). In addition, cellular levels of *psaA* mRNA were significantly reduced (Fig. 5g) whereas there was a slight increase in *psbA* mRNA (Fig. 5d).

Discussion

By probing the subcellular locations of specific mRNA molecules in two species of cyanobacteria, we have shown that the mRNAs encoding two core membrane-integral photosynthetic proteins (PsbA and PsaA) are concentrated at the inner surfaces of the thylakoid system adjacent to the central cytoplasm (Fig. 1-3). Biochemical fractionation indicates that about half of *psbA* mRNA is membrane-associated in *Synechococcus*[42]. From our images we cannot precisely quantify membrane-associated vs. cytosolic mRNA, but our results indicate that the membrane-associated

fraction must be overwhelmingly at the inner surfaces of the thylakoids. Two other mRNA species that encode proteins with other locations, the mRNAs encoding RbcL and phycocyanin subunits, are both found concentrated in spots in the central cytoplasm and are quantifiably less closely thylakoid-associated than *psbA* and *psaA* mRNAs (Fig. 4).

The locations of *psbA* and *psaA* mRNAs could in principle reflect either sites of translation or storage locations, or both. However, it is known that *psbA* mRNA in *Synechococcus* and *Synechocystis* is strongly ribosome-associated[19,20] and we found that treatment with ribosome inhibitors quantifiably changes the distribution of *psbA* and *psaA* mRNAs (Fig. 1,2). Lincomycin, which blocks translation elongation but does not detach the mRNA from the ribosome, induces dissociation of the mRNAs from the thylakoids (Figs 1,2) which is consistent with previous biochemical studies[20]. The major change in distribution of the mRNAs induced by lincomycin implies that the mRNA locations we observe reflect sites of active translation and therefore membrane insertion via the SRP-dependent pathway[17,18].

In *Synechococcus*, we were able to quantify differences in *psbA* mRNA location induced by high light treatment (Fig 2). The mRNA was always concentrated at the inner edge of the thylakoid system, but distributions varied in the extent to which the mRNA was concentrated into localised foci. In cells in standard low light conditions, *psbA* mRNA was strongly concentrated into a small number of sharp foci (Fig. 2) similarly to *psaA* mRNA (Fig. 3). In cells that had been subjected to photodamage by a short high light-treatment, *psbA* mRNA levels were higher on average, and the mRNA was much more evenly distributed over the inner edge of thylakoid (Fig. 2a,c). Under these conditions, PsbA production is predominantly implicated in PSII repair rather than *de novo* biogenesis[13], so the result suggests that *de novo* biogenesis is more localised than PSII repair. Overall, our data suggest that the first steps in photosystem biogenesis take place around the inner surfaces of the thylakoid system, adjacent to the central cytoplasm and the nucleoid. In *Synechocystis*, our results highlight the importance for biogenesis of thin extensions of the thylakoid system into the central cytoplasm. *psaA* mRNA is particularly concentrated at these extensions (Fig. 3) but they are also a major location for *psbA* mRNA (Fig. 1). Similar thylakoid extensions were not apparent in *Synechococcus*, where translation and insertion occur in discrete foci in the smooth innermost layers of the thylakoid system, with a preponderance near the cell poles (Figs 2,3). Technical constraints meant that we could not simultaneously probe

psaA and *psbA* mRNAs, and therefore it remains to be determined whether the same zones are involved in insertion of components of both photosystems.

The photosynthetic translation zones indicated by our FISH experiments match closely to the locations of thylakoid-associated ribosomes in *Synechocystis* as observed by electron tomography[6,7]. In a recent cryo-electron tomographic study, the vast majority of thylakoid-associated ribosomes were found on the inner surfaces of the thylakoid system adjacent to the central cytoplasm[7], and an earlier electron tomographic study also highlighted ribosome-covered extensions of the thylakoid system into the central cytoplasm[6]. Our results do not provide support for suggestions that photosystem biogenesis takes place initially in the plasma membrane[1,10], or in thylakoid zones immediately adjacent to the plasma membrane[7,11,15,16]. However, photosystem assembly is a complex multi-step process[12–14]. Our data only give information on sites of translation and not on the next steps of photosystem assembly, and we cannot exclude the possibility that newly-translated proteins could migrate to sites closer to the plasma membrane, where Mn integration into the PSII water-oxidising complex has been suggested to occur[15,16].

Our FISH images show that both ribosome inhibitors (Figs 1,2) and HL (Fig. 2, Extended Data Fig. 4) induce markedly different levels of *psbA* mRNA in different individual cells. The reasons remain to be determined, but it highlights variations that do not appear in bulk measurements of transcript levels. There are precedents for strong transcriptional variation among individual bacterial cells[43].

Strikingly, we found that *psbA* and *psaA* mRNAs remain concentrated near the thylakoid membrane in the presence of high concentrations of puromycin, which decouples mRNAs from the ribosomes[32] (Figs 1-3). This indicates that ribosome-uncoupled thylakoid mRNAs can be targeted to the thylakoid surface. There are precedents for such ribosome-independent mRNA targeting to membranes. In *Escherichia coli*, membrane protein mRNAs show translation-independent targeting to the plasma membrane[44]. In the chloroplast of the green alga *Chlamydomonas reinhardtii*, several mRNA species, including *psbA*, are localised at specialised translation zones around the pyrenoid by mechanisms that are partially independent of translation[44]. Translation-independent mRNA localisation in the eukaryotic cytoplasm influences the eventual destination of proteins[45]. The destination of thylakoid proteins in cyanobacteria could be strongly influenced by initial targeting of the mRNA to the thylakoid surface, prior to

ribosome association (Fig. 6). This may be the key to the unresolved membrane protein sorting problem in cyanobacteria[17].

The mechanism of membrane targeting likely involves dedicated RNA-binding proteins that recognise specific features of the mRNA molecules (Fig. 6). Indeed, we identified two *Synechocystis* RBPs that bind photosynthetic mRNAs (Fig. 5) and found that a deletion mutant lacking both these RBPs has a significant loss of thylakoid association of both *psbA* and *psaA* mRNAs (Fig. 5), accompanied by perturbations to the photosynthetic apparatus and slower growth under some conditions (Extended Data Fig. 10). Our mRNA-FISH data do not clearly show whether the RBPs simply bind the free mRNA and localise it at the membrane (as illustrated in Fig. 6) or whether they bind ribosomes and mRNA together. However, a database of protein and mRNA association in fractionated *Synechocystis* cells[46] suggests that the RBPs that we identified do not associate with the ribosome fraction, favouring the model shown in Fig. 6. Both these *Synechocystis* RBPs are partial homologs of a *Chlamydomonas* chloroplast RBP implicated in *psbA* mRNA binding and localisation at the translation zones[47]. This suggests that elements of a cyanobacterial membrane targeting system mediated by RBPs have been retained during the evolutionary transition from cyanobacteria to chloroplasts. However, much remains to be determined about the roles of different RBPs in membrane targeting, the membrane binding partners of the RBPs, and the features of specific mRNAs that they recognise.

METHODS

Strains and growth conditions

Synechocystis sp PCC 6803 (the motile PCC-M variant[22] or the glucose-tolerant GT-I[41] where specified) and *Synechococcus elongatus* PCC 7942 cells were grown in BG11 media[48] supplemented with tris(hydroxymethyl)methylamino propane sulfonic acid (TAPS), pH 8.2 at 30˚C under constant low white light (~5 µmol photons $m^{-2}s^{-1}$). Liquid cultures were maintained in tissue culture flasks (Sarstedt) with continuous shaking (130 rpm). Cultures were also maintained on BG11 plates containing 1.5% (w/v) Bacto-agar (VWR, UK) supplemented with 0.3% (w/v) $Na_2S_2O_3$. For the *Synechocystis* Δ*psbA2* mutant, media were supplemented with 25 µg ml^{-1} chloramphenicol (Sigma-Aldrich, UK), and for the *Synechocystis* triple *psbA* knockout media were supplemented with 5 mM glucose, 30 µg ml^{-1} chloramphenicol and 5 µg ml^{-1} gentamycin (Sigma-Aldrich, UK), For the *Synechocystis*

334 Δ*rbp2/3* mutant, media were supplemented with 10 µg ml^{-1} chloramphenicol and 50 µg ml^{-1} kanamycin (Carl Roth,
335 Germany). The media were additionally supplemented with 2.5 µg ml^{-1} gentamycin (Carl Roth, Germany) if used for
336 the mutant strains complemented with genes encoding proteins with a C-terminal triple FLAG-tag under control of
337 the copper inducible *petE* promoter[49]. The *Synechococcus rbcL-gfp* mutant[39,40] was grown in medium supplemented
338 with 50 µg ml^{-1} apramycin and prior to FISH measurements it was HL-treated (260 µmol photons $m^{-2}s^{-1}$ for 30-40 min
339 at 22 ˚C) to enhance *rbcL* expression[39,50]. For the affinity pull-downs and RT-qPCR, the mutants complemented with
340 FLAG-tagged versions of Rbp2 and Rbp3 were cultivated in freshwater media (50 mM $NaNO_3$, 15 mM KNO_3, 10 mM
341 $NaHCO_3$, 2.4 mM K_2HPO_4, 2 mM $MgSO_4$, 1.6 mM KH_2PO_4, 0.5 mM $CaCl_2$, 0.15 mM $FeCl_3$, 0.15 mM Na_2-EDTA, 10 µM
342 $MnCl_2$, 1 µM $ZnSO_4$, 0.1 µM Na_2MoO_4, 30 nM $CoCl_2$, 25 nM H_3BO_3) in a CellDeg system (CellDEG, Germany). The
343 cultures were supplied with 15 ml min^{-1} 10 % CO_2 and shaken at 30 °C. For the first 48h the illumination intensity was
344 set at 130 µmol photons m^{-2} s^{-1}, then increased to 250-300 µmol photons m^{-2} s^{-1} for the next 24h and then set to a
345 final illumination intensity of 700 µmol photons m^{-2} s^{-1}. The cultures were inoculated to an OD_{750} of 0.5 and protein
346 expression was induced at an OD_{750} of 8-10 by addition of 2 µM $CuSO_4$ for 24h.
347

348 **Construction of mutants**

349 The Δ*psbA2* mutant was generated in the *Synechocystis* wild type (PCC-M)[22] background by replacing the entire
350 *slr1311* (*psbA2*) gene sequence with the *cmlA* gene conferring chloramphenicol resistance (Cm^R). Cm^R was
351 introduced into the genome using a vector (pGEM-T Easy) carrying ~500 bp of *slr1311* flanking sequences either side
352 of Cm^R to assist double homologous recombination. The plasmid vector was generated by Gibson assembly[51] using
353 the NEBuilder HiFi DNA assembly master mix (NEB, UK). Primers used to amplify the DNA fragments are listed in
354 Supplementary Table 2. NEB5-alpha competent *E. coli* cells (NEB, UK) were used to clone the plasmid. *Synechocystis*
355 transformation was done following the protocol described by Clerico *et al* [52]. Successful transformation and full
356 segregation were confirmed by colony PCR (Supplementary Fig. 3). Since the Cm^R gene sequence (763 bp) is smaller
357 than *psbA2* (1083 bp), a second PCR was carried out to confirm the full segregation status of the mutant. For this
358 PCR, a primer was designed to bind within the *psbA2* sequence. Along with the reverse primer of the *psbA2*
359 downstream sequence, this *psbA2* sequence-specific primer generated an amplicon from the wild type, which was
360 absent in the mutant after full segregation (Supplementary Fig. 3).

The Δ*rbp2* disruptant was generated in the *Synechocystis* GT-I background[41] by replacing the entire target gene sequence with the drug resistance marker genes. The up- and downstream regions of the gene (*rbp2*: *ssr1480*) and the chloramphenicol resistance marker gene were amplified by PCR with respective primers (Supplementary Table 3). Amplified fragments were mixed and fused by recombinant PCR. For the construction of the *rbp3* (*slr0193*) disruptant, the DNA fragment containing the flanking regions of *rbp3* and a kanamycin-resistant gene was amplified from the genomic DNA of *rbp3* mutant (provided by Prof. Masahiko Ikeuchi). The resulting PCR products were used for the transformation of *Synechocystis* GT-I. Complete segregation was confirmed by PCR using the appropriate primers (Supplementary Table 3).

Δ*rbp* mutant strains complemented with C-terminal triple FLAG-tagged protein versions under control of the copper inducible promoter *petE* were generated by PCR amplification of the *rbp* genomic regions including their full 5' and 3'UTRs, flanked by 5' *HindII* and 3' *XhoI* restriction sites and followed by blunt end ligation into pJet1.2 (CloneJET PCR cloning kit, Thermo Fisher Scientific). The constructed vector was subjected to multiple steps of inverse PCR to introduce the bacteriophage lambda *oop* transcription terminator downstream of the 3'UTR of the respective gene and the triple FLAG tag upstream of the stop codon, followed by *DpnI* digestion (Thermo Fisher Scientific), 5' phosphorylation (T4 polynucleotide kinase, Thermo Fisher Scientific), self-ligation (T4 DNAligase, Thermo Fisher Scientific) and heat-shock transformation into chemically competent *E.coli* DH5α cells. Hereafter, the native promoter was replaced with the *petE* promoter via AQUA-cloning[53] and the final constructs were ligated into the multi-host vector pVZ322 using the *HindIII* and *XhoI* restriction sites and verified by Sanger-sequencing (GATC, Eurofins, Germany). Aliquots of 60 µL electrocompetent *Synechocystis* cells in 1 mM Hepes buffer pH 7.5 were transformed with 1 µg pVZ322 plasmid DNA by electroporation with 2.5 kV for 4 ms[54] (MicroPulser, Bio-Rad, 2 mm electrode distance), resuspended in 50 ml BG11, incubated at 30°C for 24 h, harvested and plated on BG11 agar plates, supplemented with 1 µg ml^{-1} gentamycin (Carl Roth, Germany) (Primer: Table S4).

mRNA-FISH (mRNA-Fluorescent *in situ* hybridisation)

mRNA probing was done based on the mRNA-FISH protocol described by Skinner *et al* [21] with some modifications. For each of the target mRNAs, a set of 40-48 oligonucleotide probes (each 20 nucleotides long) was designed using free online software: the Stellaris RNA FISH Probe Designer program (https://www.biosearchtech.com/stellaris-

designer). The probes were generated against the target transcript sequence, having a minimum of 2 bp inter-probe separation and a GC content of around 50%. The probe set was purchased from LGC Biosearch Technologies (California, USA and Risskov, Denmark), pre-labelled with a TAMRA (5-Carboxytetramethylrhodamine) fluorophore at the 3' end of each oligonucleotide. The probe sets used for this study are listed in Supplementary Table 1.

For the optimal detection of the photosynthetic transcripts, cultures were grown in liquid BG11 media with a starting OD (optical density) at 750 nm of 0.2. The OD of the culture was routinely measured with a UV-1800 spectrophotometer (Shimadzu). Cells were collected for mRNA-FISH when the OD_{750} reached between 0.4 and 0.6. For each sample roughly 3 x 10^8 cells were used, as calculated using a conversion factor obtained by counting cells in a haemocytometer. Cells were harvested by centrifugation (3,000x*g*, 6 minutes) and fixed immediately by treating with 1 ml PBS (Phosphate-Buffered Saline) containing 3.7% (vol/vol) formaldehyde at room temperature for 30 min. Cells were washed twice with 1 ml PBS and collected by centrifugation at 6,000x*g* for 1.5 min. The fixed cells were permeabilized with 70% ethanol for 1 h at room temperature[21]. Ethanol washed away most of the chlorophyll from the cell, which helps to reduce the background signal in the TAMRA detection channel. To achieve an even background signal from all the cells studied, an additional 2 h of 70% ethanol incubation was performed at 4 ˚C in dark. Then, cells were washed with 1 ml of 40% (w/vol) formamide, 2× SSC (Saline Sodium Citrate). The washed cell pellet was collected by centrifugation at 6,000x*g* for 1.5 min and resuspended in 25 µl hybridization buffer containing the probe set at 5 µM. The final concentration of the hybridisation buffer was adjusted to 40% (w/vol) formamide, 2× SSC, 2.5 mg dextran sulphate sodium salt, 25µg *E. coli* tRNA and 10 nM Ribonucleoside Vanadyl Complex. Hybridisation reactions were carried out overnight at 30 ˚C in the dark. Cells were then washed three times using 200 µl of 40% (w/v) formamide, 2× SSC at 30˚C with 30 minutes incubation in between each wash. The cell pellets were finally re-suspended in 50-200 µl of imaging buffer (2X SSC). Cell suspensions were spotted onto a 1.5% agarose plate (Low melt agarose, dissolved in 1X PBS). Small blocks of agar with the dried spots were cut out, mounted on a glass coverslip and placed in a custom-built sample holder for confocal imaging.

Pre-treatments before mRNA-FISH

When required, cells were treated with the inhibitors puromycin, lincomycin or rifampicin before fixation. After collecting the desired quantity of cells for mRNA-FISH, the cell pellet was resuspended in 1 ml of fresh BG11 medium containing either puromycin (500 µg ml^{-1}), lincomycin (400 µM) or rifampicin (500 µg ml^{-1}) and incubated for 1 h at

415 room temperature in ambient light (~5 µmol photons $m^{-2}s^{-1}$). For high-light (HL) treatment, the cell pellet was
416 resuspended in 1 ml BG11 medium, transferred to a 1.5 ml microfuge tube and incubated at 600 µmol photons $m^{-2}s^{-1}$
417 white light for 1h at 30 ˚C. Cells were fixed immediately after the pre-treatment, as described in the mRNA-FISH
418 section. Inhibitor experiments shown are representative of 2-3 full biological replicates.

419 **Affinity pull-downs and RT-qPCR**

420 The *Synechocystis* cultures were crosslinked with 0.1 % (v/v) formaldehyde for 15 min, The reaction was stopped by
421 addition of 125 mM glycine and incubation for 5 min. Afterwards, the cultures were washed twice with ice cold TBS
422 (150 mM NaCl, 50 mM Tris-HCl, pH 7.5) and the pellet was resuspended in 800 µl of FLAG buffer (50 mM
423 HEPES/NaOH pH 7, 5 mM $MgCl_2$, 25 mM $CaCl_2$, 150 mM NaCl, 10% [w / v] glycerol, 0.1 % Tween20) containing
424 protease inhibitor (cOmplete, Roche) and RNase inhibitor (RiboLock, Thermo Fisher Scientific). The cells were
425 mechanically disrupted with glass beads using an MM 400 (Retsch, Germany) cell disruptor. The lysate was cleared
426 from glass beads and unbroken cell debris by centrifugation at 4°C and the cleared supernatant was subjected to
427 affinity purification using 50 µl packed gel volume of FLAG M2 magnetic beads (Sigma Aldrich, Germany) and
428 incubated for 1 h at 4 °C on a rotation device. The flow-through was separated from the beads using a DynaMag-2
429 device (Thermo Fisher Scientific). Afterwards, the beads were washed six times with 20 fold packed gel volume FLAG
430 buffer + protease inhibitor and proteins were eluted by incubating twice with a 5 fold packed gel volume of 100 µg
431 $µl^{-1}$ 3xFLAG Peptide (Sigma Aldrich) for 30 min with low shaking. Both elution fractions were concentrated using
432 Amicon® Ultra 0.5 10K (Merck) concentrator columns. For subsequent RNA purification, eluates were digested by
433 proteinase K (5 % SDS, 50 mM Tris / HCl pH 7.5 and 2.5 mg/ml proteinase K) for 30 min at 30 °C, followed by addition
434 of PGTX buffer[55] and incubation at 65 °C for 15 min. Phase separation was performed by addition of
435 chloroform/isoamyl alcohol (24:1). Afterwards, the aqueous phase was mixed 1:1 with 100 % ethanol and further
436 RNA purification and DNase treatment was performed using the RNA-Clean and concentrator-5 kit (Zymo Research,
437 Germany) according to the manufacturer protocol. For the reverse transcription reaction, the QuantiTect Reverse
438 Transcription kit (Qiagen, Germany) was used. Reaction mixtures without addition of reverse transcriptase (no RT)
439 served as negative control. The qPCR was performed in a 7500 Fast Real-Time PCR system (Applied Biosystems) using
440 the Power SYBR Green PCR master mix (Applied Biosystems). All reactions were performed in triplicate for each of
441 two biological replicates. All samples were tested for the presence of residual DNA during quantitative real-time PCR
442 with an RT-minus control. The RT-qPCR data were analyzed using the 7500 software version 2.3. As endogenous

standard the RNase P RNA (*rnpB* gene) was used. *Synechocystis* cultures expressing FLAG-tagged sGFP were used as references samples for the relative quantity and therefore the relative quantity of all GFP samples were set to 1 (primers: Table S5).

Chlorophyll/OD_{750} ratio measurement, spectroscopy and growth curves

Chl concentration from whole cells was determined by diluting samples by a factor of 10 in 100% methanol, incubating at 68 ˚C for 15 minutes and pelleting insoluble material by centrifugation. Chl concentration was then calculated from the absorbance at 665 nm (UV-1800 spectrophotometer, Shimazdu) using an extinction coefficient of 12.7 $mM^{-1}cm^{-1}$ [56]. The Chl/OD ratio was obtained by dividing Chl concentration by OD_{750} measured for the culture in the same spectrophotometer. Cell absorption spectra were measured for suspensions at 3-4 µM Chl *a* with a modernised Aminco DW-2000 UV/Vis spectrophotometer (Olis, USA). Spectra were normalised to the reading at 750 nm. Fluorescence emission spectra were recorded at 77K with a Perkin-Elmer LS55 luminescence spectrometer equipped with a liquid nitrogen housing. Cells were harvested from exponential-stage cultures and resuspended to 5 µM Chl in BG11 medium. Cells were then loaded into silica capillary tubes and dark-adapted for 5 min before freezing by plunging into liquid nitrogen. Spectra were recorded for the frozen samples with excitation at 435 nm or 600 nm and emission at 620-750 nm. Excitation and emission slit-widths were 5 nm. Emission spectra were corrected for the instrument spectral response and normalised to the PSI or phycobilin fluorescence peaks after subtracting the background signal. For growth curves, technical triplicates of the *Synechocystis* cultures were grown as in "Strains and growth conditions" above except that light intensities were 50 µmol photons $m^{-2}s^{-1}$ (low light) and 80 µmol photons $m^{-2}s^{-1}$ (high light), in the presence of 10 mM glucose where specified. Optical density at 750nm was measured using a Genequant 1300 (Biochrom).

Confocal microscopy and image processing

Images were recorded with a Leica TCS-SP5 laser scanning confocal microscope equipped with a 63X oil-immersion objective (numerical aperture 1.4). The confocal pinhole was set to give a section thickness in the *z*-direction of ~0.72 µm and all images were recorded as a single slice at the same z-position. Images were recorded in 12-bit, 1024

x 1024 pixel format and acquired with 16x line averaging at 400 Hz line scan speed. Each pixel was 24 x 24 nm. For RNA-FISH samples, excitation was with a 561 nm laser source. Photosynthetic pigments were detected with an emission window of 660-700 nm, and TAMRA was detected at 565-580 nm. Live cells were imaged with excitation at 488 nm and emission 670-720 nm. Microscope control and image acquisition used Leica LAS-AF software. In all measurements, we were careful to avoid saturation of the fluorescence signal in any pixels.

Image processing was with the Fiji ImageJ package[57]. Image analysis was done after smoothing the images (below optical resolution) by blurring over a 2x2 pixel window and correcting the TAMRA channel for background autofluorescence. This was done by measuring the fluorescence in the 565-580 nm detection window relative to the signal in the 660-700 nm window for unprobed cells. The 660-700 nm image for probed cells was then multiplied by this ratio to predict the background autofluorescence image at 565-580 nm. This background image was subtracted from the observed image for probed cells to eliminate the background fluorescence. Cellular RNA-FISH signal intensities were measured using cell boundaries determined by thresholding the thylakoid (red) channel. Cells not completely in the field of view were excluded, and cells that were in contact or undergoing division were handled manually. To analyse the patchiness of the RNA-FISH signal in *Synechocystis,* cells were segmented into thylakoid and cytoplasmic regions using a level-sets plugin of Fiji ImageJ. For *Synechococcus,* patchiness was analysed by extracting a fluorescence profile from a line (8 pixels wide) drawn around the boundary between the thylakoid zone and the cytosol. In both cases, the standard deviation of the signal was measured and normalised to mean fluorescence intensity. Standard deviation and positional analyses included all cells found completely within the field of view that had a detectable FISH signal. Intensity analyses included all cells. For image presentation, the brightness of the images was adjusted at the same level for all parallel samples. Statistical significance was assessed from *p*-values obtained from two-tailed Student's t-tests, carried out with Microsoft Excel software.

Super-resolution imaging

Super-resolution spinning disc confocal fluorescence imaging was performed on a Dragonfly microscope (Andor) using super-resolution radial fluctuations (SRRF)-Stream technology[31]. A 63x oil-immersion objective (numerical aperture 1.46) and excitation at 561 nm were used. Applied settings for SRRF were: SRRF frame count=100, SRRF radiality magnification=4, SRRF ring radius=1.00 px, SRRF temporal analysis=mean, symmetrical binning 1x1. The confocal pinhole was set to 40 µm. TAMRA fluorescence was detected using a 600 nm filter (bandwidth 50 nm) and

native pigment fluorescence was detected using a 700 nm filter (bandwidth 75 nm). Images were processed with the FIJI image processing package[57].

Northern Blot analysis

RNA was isolated according to Pinto *et al.*[55], separated on a denaturing 1.3% agarose gel and blotted onto Roti-Nylon plus membrane (Carl Roth, Germany). *In vitro* transcription of PCR fragments with the Ambion T7 polymerase maxiscript kit (Thermo Fisher Scientific, Germany) and [α-^{32}P]-UTP (Hartmann Analytics, Germany) was used to generate radioactively-labeled RNA probes for the 5' UTR of *psbA2* mRNA and the control RNA RnpB. A PCR fragment covering the *psaA* sequence was labeled using the Rediprime II DNA labeling system (GE Healthcare Life Sciences). Hybridization signals were detected on a Typhoon FLA4500 imaging system (GE Healthcare) and quantified using Quantity One software (Bio-Rad Laboratories, Germany). Primers used to amplify PCR products for labeling reactions are given in Supplementary Table 6.

Antiserum against *Synechocystis* Rbp3 protein.

For the expression of 6×His-tagged Rbp3 protein, the PCR-amplified *rbp3* gene was cloned into pETNH vector[58] using In-Fusion Cloning kit (TaKaRa, Shiga, Japan). After verification of the sequences, the plasmids were introduced into *E. coli* Rosetta competent cells (TaKaRa) and used for the purification of recombinant Rbp3 proteins as follows. The resulting *E. coli* strain was grown in 100 ml of LB medium at 37°C. When the culture reached an OD_{600} of 0.5, IPTG was added to medium at a final concentration of 1 mM and the growing temperature was shifted to 20°C. After 24 h, cells were harvested by centrifugation, washed with a purification buffer (20 mM Tris-HCl (pH 8.0 at 4°C) and 250 mM NaCl), and stored at −80°C until use. For protein purification, frozen cells were suspended in 5 ml of purification buffer containing 1 mM PMSF. The cells were disrupted by sonication and centrifugated at 15,000 × g for 30 min at 4°C, the resulting supernatant was mixed with 1 ml of Ni^{2+}-NTA agarose resin (QIAGEN) equilibrated with purification buffer and loaded onto a column. After washing by 10 ml of washing buffer 1 [20 mM Tris-HCl (pH 8.0), 250 mM NaCl, and 5 mM imidazole] and 50 ml of washing buffer 2 [20 mM Tris-HCl (pH 8.0 at 4°C), 250 mM NaCl, and 20 mM imidazole], proteins were then eluted with 10 ml of an elution buffer [20 mM Tris-HCl (pH 8.0 at 4°C), 250 mM NaCl, and 200 mM imidazole], and dialyzed against the dialysis buffer [20 mM HEPES (pH 7.5), 5 mM $MgSO_4$, 1 mM EDTA, 0.0001% (w/v) BSA, 0.05% Tween 20, 150 mM NaCl, and 30% Glycerol]. The purity of the protein was confirmed by

SDS–PAGE, and a polyclonal antibody to the protein was generated by immunising a rabbit (Eurofins, Ebersberg, Germany).

Cell fractionation and Western blotting.

Exponential phase cells of *Synechocystis* PCC-M strain were harvested and subjected to fractionation according to the procedure described previously[20] except for the polysome isolation. After the fractionation, crude extracts were prepared using 10% trichloroacetic acid as described previously[59]. 25 µg and 15 µg of samples were analysed by Western blotting using anti-Rbp3 and anti-RbcL (Agrisera) antibodies as the primary antibody (dilution 2000x), and HRP-conjugated anti-rabbit IgG antibody (GE Healthcare) as the secondary antibody (dilution 10000x).

REFERENCES

1. Pisareva, T. *et al.* Model for membrane organization and protein sorting in the cyanobacterium *Synechocystis* sp. PCC 6803 inferred from proteomics and multivariate sequence analyses. *J. Proteome Res.* **10**, 3617–3631 (2011).
2. Mullineaux, C. W. Co-existence of photosynthetic and respiratory activities in cyanobacterial thylakoid membranes. *Biochim. Biophys. Acta - Bioenerg.* **1837**, 503–511 (2014).
3. Baers, L. L. *et al.* Proteome mapping of a cyanobacterium reveals distinct compartment organization and cell-dispersed metabolism. *Plant Physiol.* **181**, 1721–1738 (2019).
4. Nevo, R. *et al.* Thylakoid membrane perforations and connectivity enable intracellular traffic in cyanobacteria. *EMBO J.* **26**, 1467–1473 (2007).
5. Liberton, M., Austin, J. R., Berg, R. H. & Pakrasi, H. B. Unique thylakoid membrane architecture of a unicellular N_2-fixing cyanobacterium revealed by electron tomography. *Plant Physiol.* **155**, 1656–1666 (2011).
6. van de Meene, A. M. L., Hohmann-Marriott, M. F., Vermaas, W. F. J. & Roberson, R. W. The three-dimensional structure of the cyanobacterium *Synechocystis* sp. PCC 6803. *Arch. Microbiol.* **184**, 259–270 (2006).
7. Rast, A. *et al.* Biogenic regions of cyanobacterial thylakoids form contact sites with the plasma membrane. *Nat. Plants* **5**, 436–446 (2019).
8. Mullineaux, C. W. & Liu, L.-N. Membrane dynamics in phototrophic bacteria. *Annu. Rev. Microbiol.* **74**, 633–654 (2020).
9. Zhao, L.-S. *et al.* Structural variability, coordination, and adaptation of a native photosynthetic machinery. *Nat. Plants* **6**, 869–882 (2020).
10. Zak, E. *et al.* The initial steps of biogenesis of cyanobacterial photosystems occur in plasma membranes. *Proc. Natl. Acad. Sci.* **98**, 13443–13448 (2001).
11. Selão, T. T., Zhang, L., Knoppová, J., Komenda, J. & Norling, B. Photosystem II assembly steps take place in the thylakoid membrane of the cyanobacterium *Synechocystis* sp. PCC6803. *Plant Cell Physiol.* **57**, 95–104 (2015).
12. Heinz, S., Liauw, P., Nickelsen, J. & Nowaczyk, M. Analysis of photosystem II biogenesis in cyanobacteria. *Biochim. Biophys. Acta - Bioenerg.* **1857**, 274–287 (2016).
13. Nixon, P. J., Michoux, F., Yu, J., Boehm, M. & Komenda, J. Recent advances in understanding the assembly and repair of photosystem II. *Ann. Bot.* **106**, 1–16 (2010).
14. Chidgey, J. W. *et al.* A cyanobacterial chlorophyll synthase-HliD complex associates with the Ycf39 protein and the YidC/Alb3 insertase. *Plant Cell* **26**, 1267–1279 (2014).

15. Rengstl, B., Oster, U., Stengel, A. & Nickelsen, J. An intermediate membrane subfraction in cyanobacteria is involved in an assembly network for Photosystem II biogenesis. *J. Biol. Chem.* **286**, 21944–21951 (2011).

16. Stengel, A. *et al.* Initial steps of Photosystem II *de novo* assembly and preloading with manganese take place in biogenesis centers in *Synechocystis*. *Plant Cell* **24**, 660–675 (2012).

17. Frain, K. M., Gangl, D., Jones, A., Zedler, J. A. Z. & Robinson, C. Protein translocation and thylakoid biogenesis in cyanobacteria. *Biochim. Biophys. Acta - Bioenerg.* **1857**, 266–273 (2016).

18. Luirink, J. & Sinning, I. SRP-mediated protein targeting: structure and function revisited. *Biochim. Biophys. Acta - Mol. Cell Res.* **1694**, 17–35 (2004).

19. Mulo, P., Sakurai, I. & Aro, E.-M. Strategies for psbA gene expression in cyanobacteria, green algae and higher plants: From transcription to PSII repair. *Biochim. Biophys. Acta - Bioenerg.* **1817**, 247–257 (2012).

20. Tyystjärvi, T., Herranen, M. & Aro, E.-M. Regulation of translation elongation in cyanobacteria: membrane targeting of the ribosome nascent-chain complexes controls the synthesis of D1 protein. *Mol. Microbiol.* **40**, 476–484 (2001).

21. Skinner, S. O., Sepúlveda, L. A., Xu, H. & Golding, I. Measuring mRNA copy number in individual *Escherichia coli* cells using single-molecule fluorescent *in situ* hybridization. *Nat. Protoc.* **8**, 1100–1113 (2013).

22. Trautmann, D., Voß, B., Wilde, A., Al-Babili, S. & Hess, W. R. Microevolution in cyanobacteria: Re-sequencing a motile substrain of *Synechocystis* sp. PCC 6803. *DNA Res.* **19**, 435–448 (2012).

23. Mullineaux, C. W. & Sarcina, M. Probing the dynamics of photosynthetic membranes with fluorescence recovery after photobleaching. *Trends Plant Sci.* **7**, 237–240 (2002).

24. Liu, L.-N. Distribution and dynamics of electron transport complexes in cyanobacterial thylakoid membranes. *Biochim. Biophys. Acta - Bioenerg.* **1857**, 256–265 (2016).

25. Liu, L.-N. *et al.* Control of electron transport routes through redox-regulated redistribution of respiratory complexes. *Proc. Natl. Acad. Sci.* **109**, 11431–11436 (2012).

26. Casella, S. *et al.* Dissecting the native architecture and dynamics of cyanobacterial photosynthetic machinery. *Mol. Plant* **10**, 1434–1448 (2017).

27. Mohamed, A., Eriksson, J., Osiewacz, H. D. & Jansson, C. Differential expression of the *psbA* genes in the cyanobacterium *Synechocystis* 6803. *Mol. Gen. Genet. MGG* **238**, 161–168 (1993).

28. Kulkarni, R. D., Schaefer, M. R. & Golden, S. S. Differential expression of members of a cyanobacterial *psbA* gene family in response to light. *J. Bacteriol.* **171**, 3973–3981 (1989).

29. Debus, R. J., Nguyen, A. P. & Conway, A. B. Identification of ligands to manganese and calcium in Photosystem II by site-directed mutagenesis. in *Current Research in Photosynthesis.* (ed. Baltscheffsky, M.) 829–832 (Springer Netherlands, 1990). doi:10.1007/978-94-009-0511-5_191

30. Schuergers, N. *et al.* Cyanobacteria use micro-optics to sense light direction. *Elife* **5**, e12620 (2016).

31. Gustafsson, N. *et al.* Fast live-cell conventional fluorophore nanoscopy with ImageJ through super-resolution radial fluctuations. *Nat. Commun.* **7**, 12471 (2016).

32. Salem, K. & van Waasbergen, L. G. Photosynthetic electron transport controls expression of the High Light Inducible gene in the cyanobacterium *Synechococcus elongatus* strain PCC 7942. *Plant Cell Physiol.* **45**, 651–658 (2004).

33. Herranen, M., Aro, E. & Tyystja, T. Two distinct mechanisms regulate the transcription of photosystem II genes in *Synechocystis* sp PCC6803. *Plant Cell* 531–539 (2001).

34. Constant, S., Perewoska, I., Alfonso, M. & Kirilovsky, D. Expression of the *psbA* gene during photoinhibition and recovery in *Synechocystis* PCC 6714: Inhibition and damage of transcriptional and translational machinery prevent the restoration of photosystem II activity. *Plant Mol. Biol.* **34**, 1–13 (1997).

35. Olive, J., Ajlani, G., Astier, C., Recouvreur, M. & Vernotte, C. Ultrastructure and light adaptation of

phycobilisome mutants of *Synechocystis* PCC 6803. *Biochim. Biophys. Acta - Bioenerg.* **1319**, 275–282 (1997).

36. Savage, D. F., Afonso, B., Chen, A. H. & Silver, P. A. Spatially ordered dynamics of the bacterial carbon fixation machinery. *Science* **327**, 1258–1261 (2010).

37. Faulkner, M. *et al.* Direct characterization of the native structure and mechanics of cyanobacterial carboxysomes. *Nanoscale* **9**, 10662–10673 (2017).

38. Sun, Y., Wollman, A. J. M., Huang, F., Leake, M. C. & Liu, L.-N. Single-organelle quantification reveals stoichiometric and structural variability of carboxysomes dependent on the environment. *Plant Cell* **31**, 1648–1664 (2019).

39. Sun, Y. *et al.* Light modulates the biosynthesis and organization of cyanobacterial carbon fixation machinery through photosynthetic electron flow. *Plant Physiol.* **171**, 530–541 (2016).

40. Huang, F. *et al.* Roles of RbcX in carboxysome biosynthesis in the cyanobacterium *Synechococcus elongatus* PCC7942. *Plant Physiol.* **179**, 184–194 (2019).

41. Kanesaki, Y. *et al.* Identification of substrain-specific mutations by massively parallel whole-genome resequencing of *Synechocystis* sp. PCC 6803. *DNA Res.* **19**, 67–79 (2011).

42. Tyystjärvi, T., Sirpiö, S. & Aro, E.-M. Post-transcriptional regulation of the *psbA* gene family in the cyanobacterium *Synechococcus* sp. PCC 7942. *FEBS Lett.* **576**, 211–215 (2004).

43. Elowitz, M. B., Levine, A. J., Siggia, E. D. & Swain, P. S. Stochastic gene expression in a single cell. *Science* **297**, 1183–1186 (2002).

44. Nevo-Dinur, K., Nussbaum-Shochat, A., Ben-Yehuda, S. & Amster-Choder, O. Translation-independent localization of mRNA in *E. coli*. *Science* **331**, 1081–4 (2011).

45. Weis, B. L., Schleiff, E. & Zerges, W. Protein targeting to subcellular organelles via mRNA localization. *Biochim. Biophys. Acta - Mol. Cell Res.* **1833**, 260–273 (2013).

46. Riediger, M., Spät, P., Bilger, R., Macek, B. & Hess, W. R. Analysis of a photosynthetic cyanobacterium rich in internal membrane systems via gradient profiling by sequencing (Grad-seq). *bioRxiv* 2020.07.02.184192 (2020). doi:10.1101/2020.07.02.184192

47. Uniacke, J. & Zerges, W. Chloroplast protein targeting involves localized translation in *Chlamydomonas*. *Proc. Natl. Acad. Sci. U. S. A.* **106**, 1439–1444 (2009).

48. Castenholz, R. W. Culturing methods for cyanobacteria. *Methods Enzymol.* **167**, 68–93 (1988).

49. Zhang, L., McSpadden, B., Pakrasi, H. B. & Whitmarsh, J. Copper-mediated regulation of cytochrome c_{553} and plastocyanin in the cyanobacterium *Synechocystis* 6803. *J. Biol. Chem.* **267**, 19054–19059 (1992).

50. Kopf, M. *et al.* Comparative analysis of the primary transcriptome of *Synechocystis* sp. PCC 6803. *DNA Res.* **21**, 527–539 (2014).

51. Gibson, D. G. *et al.* Enzymatic assembly of DNA molecules up to several hundred kilobases. *Nat. Methods* **6**, 343–345 (2009).

52. Clerico, E. M., Ditty, J. L. & Golden, S. S. Specialized techniques for site-directed mutagenesis in cyanobacteria. in *Circadian rhythms: methods and protocols* (ed. Rosato, E.) 155–171 (Humana Press, 2007). doi:10.1007/978-1-59745-257-1_11

53. Beyer, H. M. *et al.* AQUA Cloning: A Versatile and Simple Enzyme-Free Cloning Approach. *PLoS One* **10**, e0137652–e0137652 (2015).

54. Ferreira, E. A. *et al.* Expanding the toolbox for *Synechocystis* sp. PCC 6803: validation of replicative vectors and characterization of a novel set of promoters. *Synth. Biol.* **3**, ysy014 (2018).

55. Pinto, F. L., Thapper, A., Sontheim, W. & Lindblad, P. Analysis of current and alternative phenol based RNA extraction methodologies for cyanobacteria. *BMC Mol. Biol.* **10**, 1–8 (2009).

56. Meeks, J. C. & Castenholz, R. W. Growth and photosynthesis in an extreme thermophile, *Synechococcus*

lividus (Cyanophyta). *Arch. Mikrobiol.* **78**, 25–41 (1971).

57. Schindelin, J. *et al.* Fiji - an Open platform for biological image analysis. *Nat. Methods* **9**, 241 (2009).

58. Watanabe, S., Sato, M., Nimura-Matsune, K., Chibazakura, T. & Yoshikawa, H. Protection of psbAII transcript from ribonuclease degradation in vitro by DnaK2 and DnaJ2 chaperones of the cyanobacterium Synechococcus elongatus PCC 7942. *Biosci. Biotechnol. Biochem.* **71**, 279–282 (2007).

59. Nimura, K., Takahashi, H. & Yoshikawa, H. Characterization of the *dnaK* multigene family in the cyanobacterium *Synechococcus* sp. strain PCC7942. *J. Bacteriol.* **183**, 1320–1328 (2001).

DATA AVAILABILITY

The datasets analysed during the current study are available from the corresponding author on reasonable request.

ACKNOWLEDGEMENTS

We acknowledge support from the European Union's Horizon 2020 research and innovation programme under Marie Sklodowska Curie Grant Agreement 675006 (SE2B), Biotechnology and Biological Sciences Research Council Grants BB/P001807/1 and BB/R003890/1, Biotechnology and Biological Sciences Research Council ALERT17 grant BB/R01390X/1, Royal Society University Research Fellowships UF120411 and URF\R\180030 to L-NL and Deutsche Forschungsgemeinschaft Research Training Group MeInBio - 322977937/GRK2344 to AW and WRH. We thank Werner Bigott (University of Freiburg) for Northern blot analysis, the Liverpool Centre for Cell Imaging for technical assistance and equipment provision, and Joko Trinugoho and Peter Nixon (Imperial College London) for supplying the *Synechocystis psbA* triple mutant (originally from Richard Debus, University of California Riverside).

AUTHOR CONTRIBUTIONS

MM carried out the bulk of the experimental work and data analysis. LH, MR, SW and WRH generated and characterised RBP mutants and analysed RBP-mRNA association. YY and RK carried out *cpcAB* and *rbcL* FISH measurements. HC assisted with data analysis. CE helped to establish the RNA-FISH technique in the lab and discussed data. TH and L-NL performed super-resolution microscopy and data analysis and provided the *rbcL-gfp* mutant. AW designed and analysed Northern Blot hybridisation experiments and discussed data. CWM and MM devised the study and wrote the paper, with input from all authors.

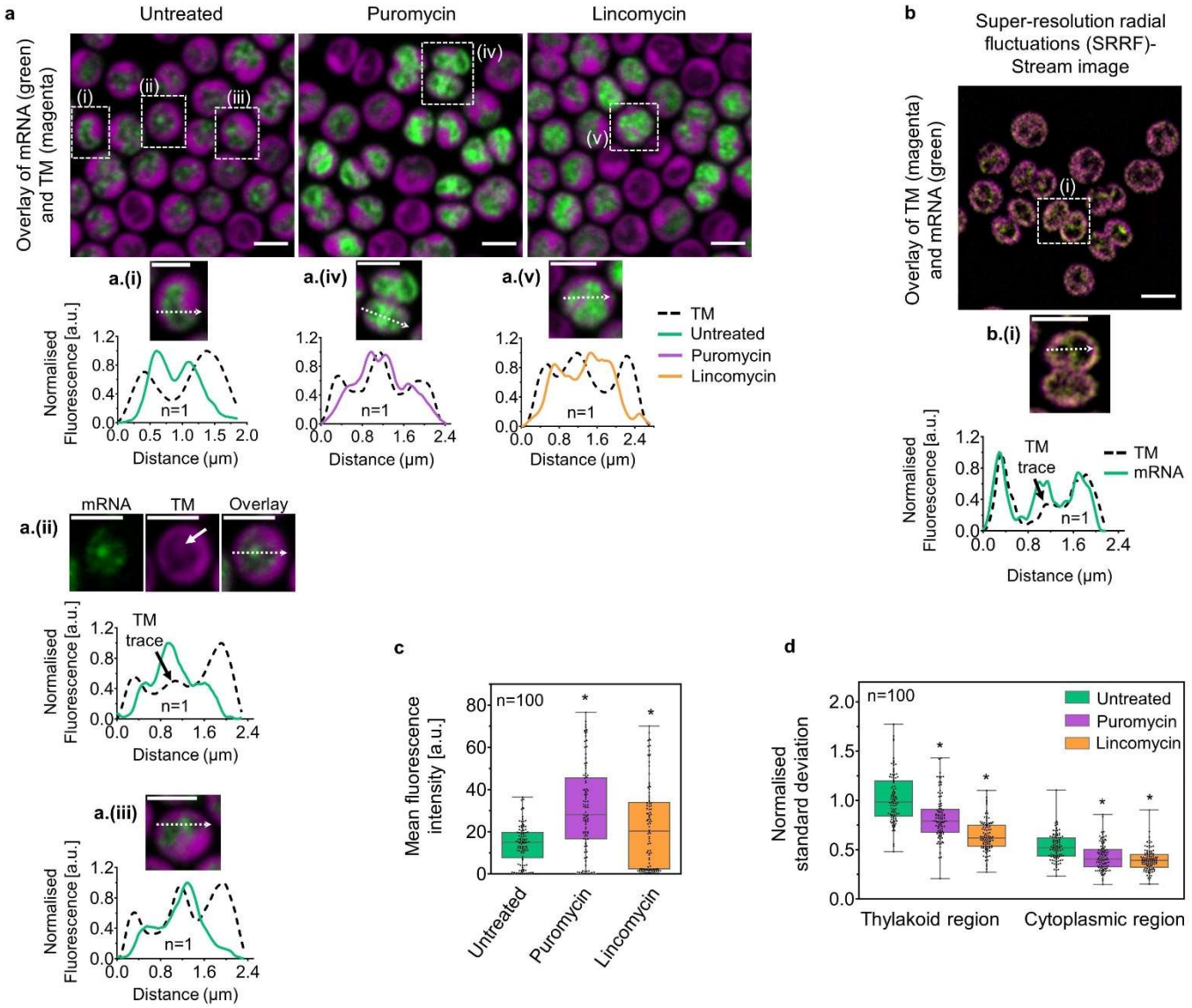

Figure 1: Location of mRNAs encoding PsbA proteins in *Synechocystis*, with effects of ribosome inhibitors. a, *Synechocystis psbA* mRNA (green) relative to thylakoid membrane (magenta) with and without pre-exposure to puromycin and lincomycin. Representative cells (**a,** i-v) are shown in enlarged form below the corresponding micrographs. Line profiles from the representative cells (**a,** i-v) show location of transcript signal relative to thylakoid membrane (TM). **b,** Super-resolution fluorescence image showing the localisation of *psbA* mRNA relative to TM. Line profile of a representative cell (**b,** i) shows a TM projection (arrow) coinciding with the mRNA peak in the middle of the cell. **c,d**, Quantitation of inhibitor effects on *psbA* mRNAs, showing relative FISH signal per cell (c: p=2x10^{-11} for puromycin vs untreated, 3x10^{-4} for lincomycin vs untreated) and the patchiness of its subcellular distribution, assessed by the normalised standard deviation in the FISH signal (d: in thylakoids p=2x10^{-8} for puromycin vs. untreated, 4x10^{-27} for lincomycin vs untreated; in cytoplasm p=5x10^{-7} for puromycin vs. untreated, 4x10^{-12} for lincomycin vs untreated). Error bars in the box plots indicate the range of values recorded, the centre line shows the

688 median and the box spans the interquartile range. n: number of cells measured, *: significant difference from the

689 untreated cells, at $p < 0.001$, measured by unpaired two-tailed Student's t-test. All scale bars: 2µm.

690

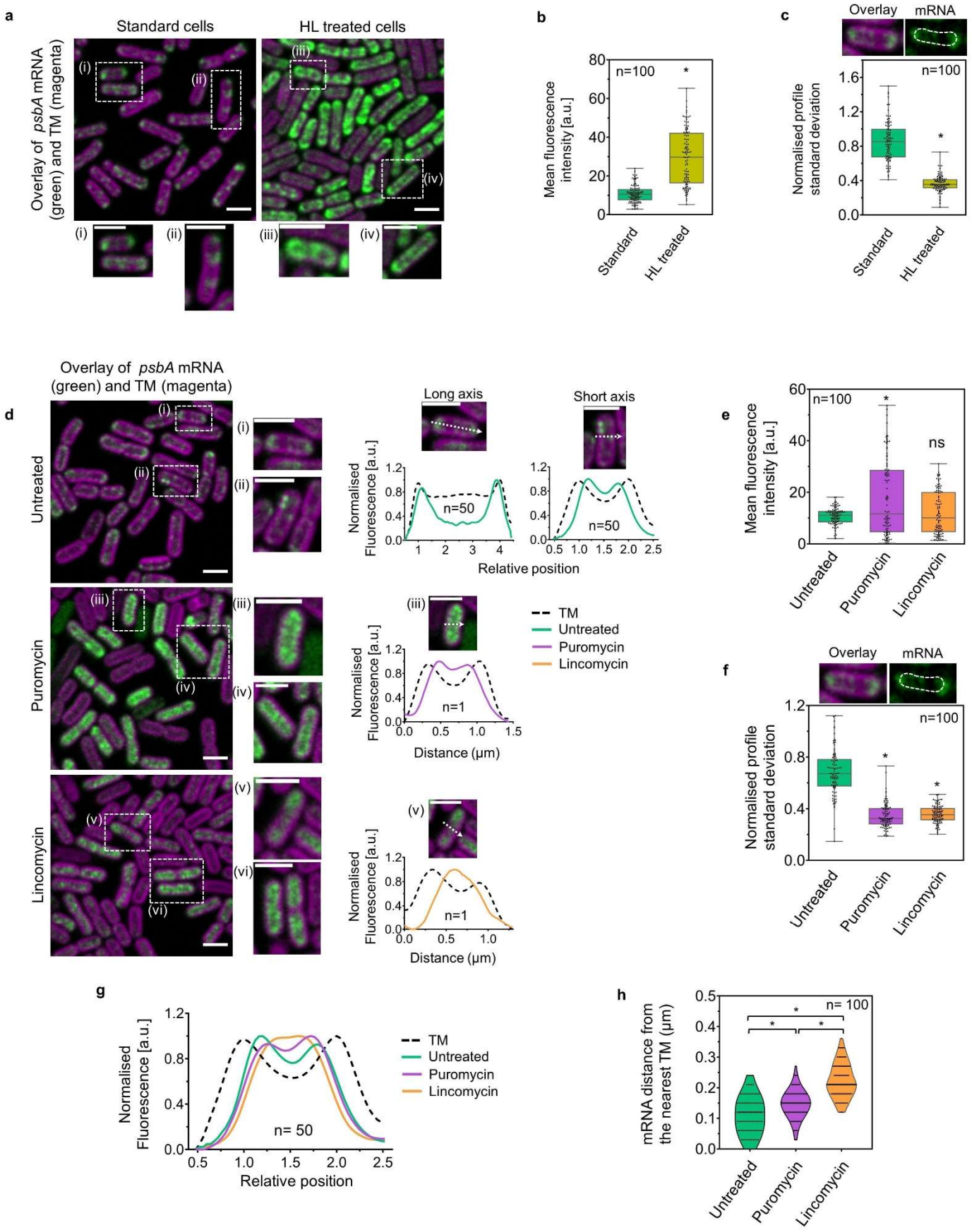

691

692 **Figure 2: Distribution of *psbA* mRNA in *Synechococcus* under different conditions**. **a-c**, Abundance and

693 distribution of *psbA* mRNA, comparing standard conditions with high light-treated cells (HL, 600 µmol photons $m^{-2}s^{-1}$,

694 1h); **a,** Micrographs of the cells showing mRNA in green and thylakoid membrane (TM) in magenta; **b,** relative mRNA

695 signals per cell (p=8x10^{-15}); **c,** Patchiness of mRNA distribution, assessed by measuring the standard deviation in the

696 FISH signal along a profile drawn around the TM as shown (p=2x10^{-40}); **d-h,** Effects of ribosome inhibitors; **d,**
697 Fluorescence micrographs: representative cells are shown enlarged at the right of corresponding micrograph. Line
698 profiles from each of the samples are presented next to the enlarged micrographs, showing mRNA signal relative to
699 TM. For untreated cells, long-axis and short-axis line profiles are averaged from 50 cells; for puromycin and
700 lincomycin, line profiles next to the enlarged micrographs are drawn from a single representative cell; **e,f,**
701 Quantitation of inhibitor effects showing relative FISH signal intensity (p=10^{-5} for untreated vs puromycin, 0.18 for
702 untreated vs lincomycin) (e) and the patchiness of the mRNA distribution (p=2x10^{-29} for untreated vs puromycin,
703 2x10^{-28} for untreated vs lincomycin) (f). **g,** averaged line profiles across the short axis of the cells showing effects of
704 inhibitors on the subcellular distribution of mRNA; **h,** Distance of mRNA from the nearest TM. Peak-to-peak distances
705 measured from short-axis line profiles (p= 3x10^{-6} for untreated vs puromycin, 8x10^{-30} for untreated vs lincomycin,
706 7x10^{-21} for puromycin vs lincomycin). The thick line at the middle of each violin plot shows the median. Error bars in
707 the box plots indicate the range of values recorded, the centre line shows the median and the box spans the
708 interquartile range. n: number of cells measured for b, c, e, f and number of mRNA peaks measured for h, *:
709 significant difference from the condition shown at the left of the plot, at p< 0.001, measured by unpaired two-tailed
710 Student's t-test; ns: p-value non-significant. All scale bars: 2 µm
711

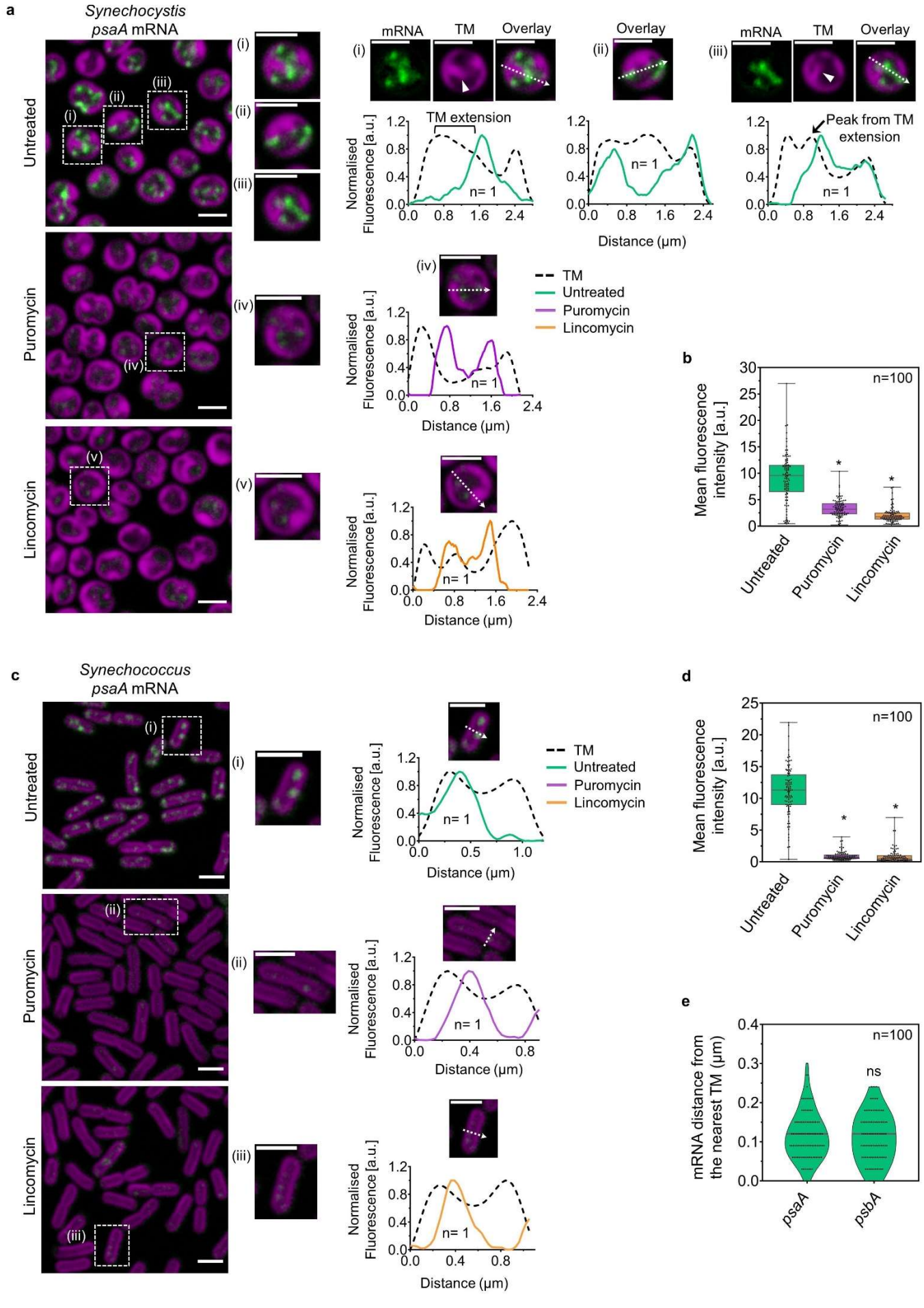
a
Synechocystis
psaA mRNA
Untreated
Puromycin
Lincomycin
(i)
(ii)
(iii)
(iv)
(v)
mRNA
TM
Overlay
TM extension
Peak from TM extension
Normalised Fluorescence [a.u.]
Distance (μm)
n= 1
TM
Untreated
Puromycin
Lincomycin
b
Mean fluorescence intensity [a.u.]
n=100
Untreated
Puromycin
Lincomycin
c
Synechococcus
psaA mRNA
d
e
mRNA distance from the nearest TM (μm)
ns
psaA
psbA

Figure 3: Location of mRNAs encoding PsaA proteins in *Synechocystis* and *Synechococcus*, with effects of ribosome inhibitors. a, *psaA* mRNA FISH signal (green) in *Synechocystis* relative to thylakoid membrane (magenta) ± inhibitor pre-treatment. Representative cells (a, i-v) are shown in enlarged form at the right of the corresponding micrographs. Line profiles from the representative cells (a, i-v) show location of transcript signal relative to thylakoid membrane (TM). Thylakoid extension towards the cytoplasm is marked with arrowheads **b,** Quantitation of effects of inhibitors on the mean FISH signal per cell in *Synechocystis* (p=4x10^{-21} for puromycin vs untreated, 2x10^{-27} for lincomycin vs untreated). **c,** *psaA* mRNA FISH signal (green) in *Synechococcus* relative to thylakoid membrane (magenta) ± inhibitor pre-treatment: enlarged examples shown below with line profiles. **d,** Quantitation of effects of inhibitors on the mean FISH signal per cell in *Synechococcus* (p=2x10^{-47} for puromycin vs untreated, 5x10^{-49} for lincomycin vs untreated). **e,** Comparison of the distance of mRNA FISH signals from the closest TM for *psbA* and *psaA* in *Synechococcus* (p= 0.5). Detail of the *psbA* mRNA of *Synechococcus* is shown in Fig. 2. The thick line at the middle of each violin plot represents the median). Error bars in the box plots indicate the range of values recorded, the centre line shows the median and the box spans the interquartile range. n: number of cells measured, *: significant difference from the untreated cells, at p< 0.001, measured by unpaired two-tailed Student's t-test; ns: p-value non-significant; all scale bars: 2µm.

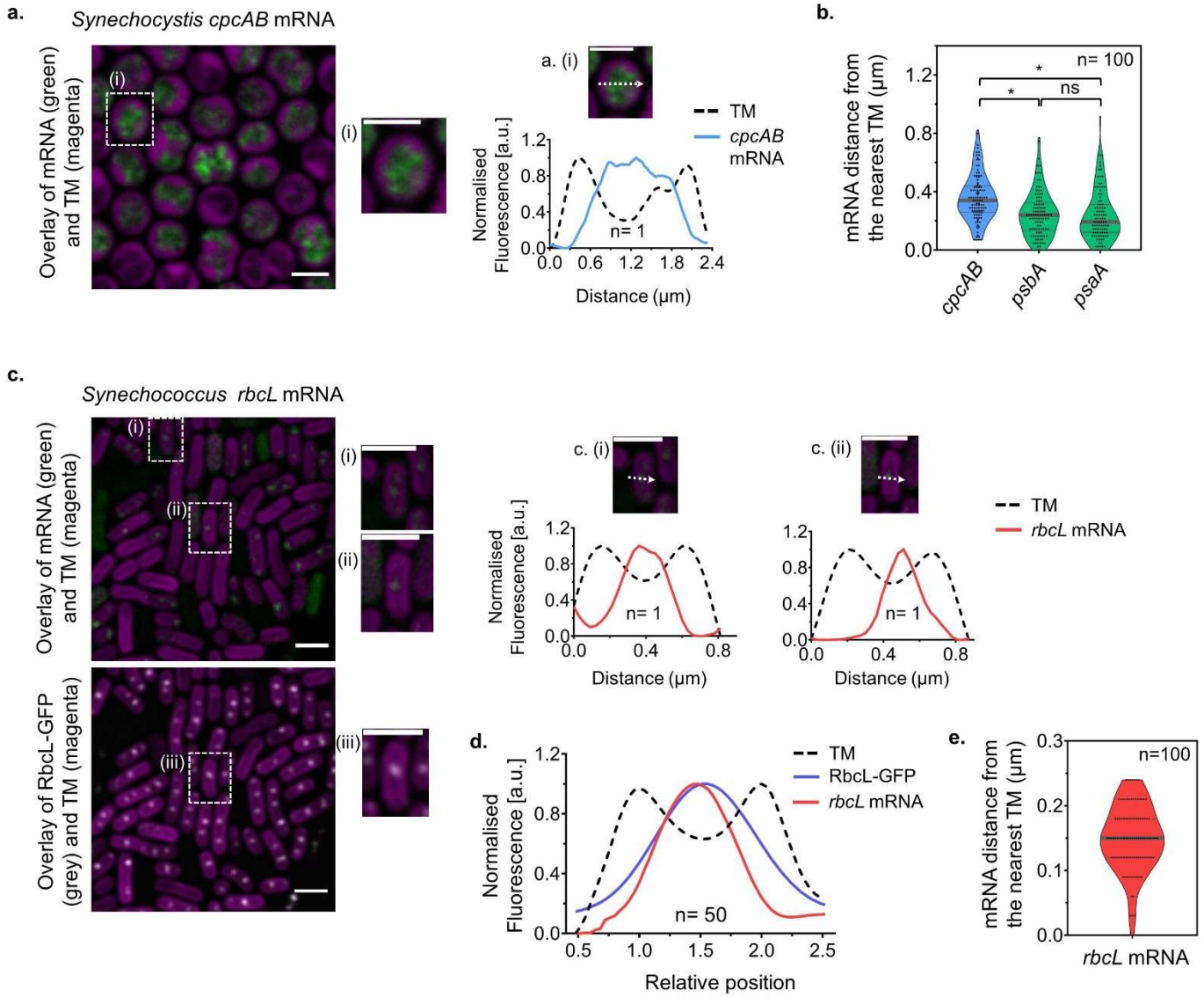

729

730 **Figure 4: Location of mRNAs that do not encode TM-integral proteins: *cpcAB* in *Synechocystis* and *rbcL* in**

731 ***Synechococcus*. a,** *cpcAB* mRNA FISH signal (green) in *Synechocystis* relative to thylakoid membrane (magenta).

732 Representative cell (a, i) is shown in enlarged form at the right of the micrograph. Line profile from the

733 representative cell show location of transcript signal relative to thylakoid membrane (TM). **b,** Comparison of the

734 distance of mRNA FISH signals from the closest TM for three mRNA species: *cpcAB, psbA* and *psaA* in *Synechocystis*

735 (p=7x10^{-7} for *cpcAB* vs *psbA*, 9x10^{-7} for *cpcAB* vs *psaA,* 0.72 for *psbA* vs *psaA*). The thick line at the middle of each

736 violin plot represents the median. n: number of cells measured. *: significant difference (p< 0.001), measured by

737 unpaired two-tailed Student's t-test; ns: p-value non-significant. **c,** *rbcL* mRNA FISH signal (green: top) and RbcL-GFP

738 signal (grey: bottom) in *Synechococcus* relative to thylakoid membrane (magenta). Representative cells (c, i-iii) are

739 shown in enlarged form at the right of the micrograph. Short-axis line profiles from representative cells (c, i-ii) show

740 location of transcript signal relative to TM. **d,** Averaged short-axis line profiles showing the distributions of *rbcL*

741 mRNA and RbcL-GFP relative to TM in *Synechococcus.* **e,** Violin plot showing distance from *rbcL* mRNA

concentrations to the nearest TM. *n* = 100 cells. *rbcL* mRNA is significantly further from the TM than *psbA* mRNA and *psaA* mRNA (Fig. 3e: *p* from two-tailed Student's t-tests = 10^{-6} for *psbA* and 10^{-5} for *psaA*). All scale-bars: 2µm.

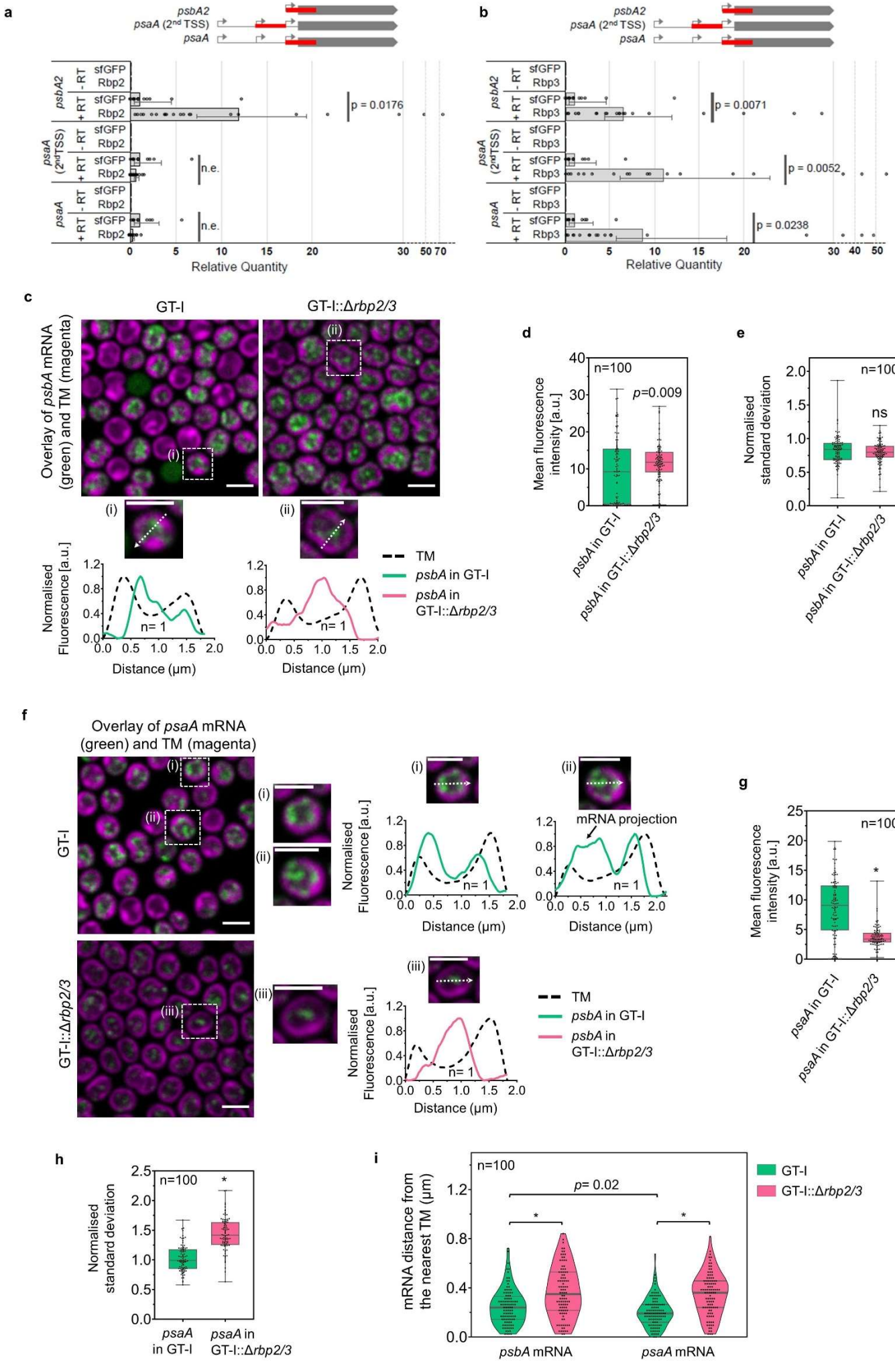
a
psbA2
psaA (2nd TSS)
psaA
psbA2
psaA (2nd TSS)
psaA
+ RT
- RT
sfGFP
Rbp2
p = 0.0176
n.e.
n.e.
0
5
10
15
20
30
50
70
Relative Quantity
b
psbA2
psaA (2nd TSS)
psaA
Rbp3
p = 0.0071
p = 0.0052
p = 0.0238
0
5
10
15
20
30
40
50
Relative Quantity
c
GT-I
GT-I::Δrbp2/3
Overlay of psbA mRNA (green) and TM (magenta)
(i)
(ii)
Normalised Fluorescence [a.u.]
n= 1
Distance (μm)
TM
psbA in GT-I
psbA in GT-I::Δrbp2/3
d
Mean fluorescence intensity [a.u.]
n=100
p=0.009
psbA in GT-I
psbA in GT-I::Δrbp2/3
e
Normalised standard deviation
n=100
ns
psbA in GT-I
psbA in GT-I::Δrbp2/3
f
Overlay of psaA mRNA (green) and TM (magenta)
GT-I
GT-I::Δrbp2/3
(i)
(ii)
(iii)
mRNA projection
n= 1
Distance (μm)
TM
psbA in GT-I
psbA in GT-I::Δrbp2/3
g
Mean fluorescence intensity [a.u.]
n=100
psaA in GT-I
psaA in GT-I::Δrbp2/3
h
Normalised standard deviation
n=100
psaA in GT-I
psaA in GT-I::Δrbp2/3
i
mRNA distance from the nearest TM (μm)
n=100
p= 0.02
GT-I
GT-I::Δrbp2/3
psbA mRNA
psaA mRNA

Figure 5: RNA-binding proteins in *Synechocystis* GT-I and their effects on mRNA localisation. a,b, RT-qPCR analysis of *psbA2, psaA* and *psaA* proximal 5' UTR (2nd TSS) mRNA binding to FLAG-tagged RBP2 (a) and RBP3 (b), with FLAG-tagged GFP as negative control and *rnpB* as endogenous control for normalisation. *n* = 6 for all data (triplicate reactions from 2 biological replicates). Error bars in in RT-qPCR represent the mean of the minimum and maximum relative quantities from all measurements. Asterisks label significant difference from the sfGFP control, at $p < 0.05$, measured by unpaired two-tailed Student's t-test. n.e.: not enriched. **c,** Micrographs showing *psbA* mRNA (green) location relative TM (magenta) in GT-I and GT-I::*Δrbp2/3*. Representative cells (**c. i and ii)** are shown in enlarged form below the corresponding micrographs. Line profiles from the representative cells show location of transcript signal relative to thylakoid membrane (TM). **d,** Relative *psbA* mRNA signal intensity in GT-I and ΔGT-I::Δ*rbp2/3* cells. **e,** patchiness of the *psbA* mRNA distribution patterns assessed from normalised standard deviation in the signal ($p = 0.28$). **f,** Micrographs showing *psaA* mRNA (green) location relative to TM (magenta) in GT-I and ΔGT-1::Δ*rbp2/3*. Representative cells (**f. i-iii)** are shown in enlarged form at the right of the corresponding micrographs. Line profiles from the representative cells show location of transcript signal relative to TM. **g,** Relative *psaA* mRNA signal intensity in GT-I and ΔGT-I::Δ*rbp2/3* cells ($p = 4 \times 10^{-16}$). **h,** patchiness of *psaA* mRNA distribution assessed from the standard deviation in the FISH image, ($p = 6 \times 10^{-21}$ for GT-I vs. ΔGT-I::Δ*rbp2/3*). **i,** Violin plot comparing the distance of *psbA* and *psaA* mRNA spots from the closest thylakoid membrane in GT-I vs. GT-I::Δ*rbp2/3* ($p = 7 \times 10^{-6}$ for *psbA* mRNA; 2×10^{-10} for *psaA* mRNA). The thick grey line in each violin plot represents the median distance to TM. Error bars in the box plots indicate the range of values recorded, the centre line shows the median and the box spans the interquartile range. n: number of cells measured, *: significant difference from the untreated cells, at $p < 0.001$, measured by unpaired two-tailed Student's t-test; ns: *p*-value non-significant; scale bars: 2μm.

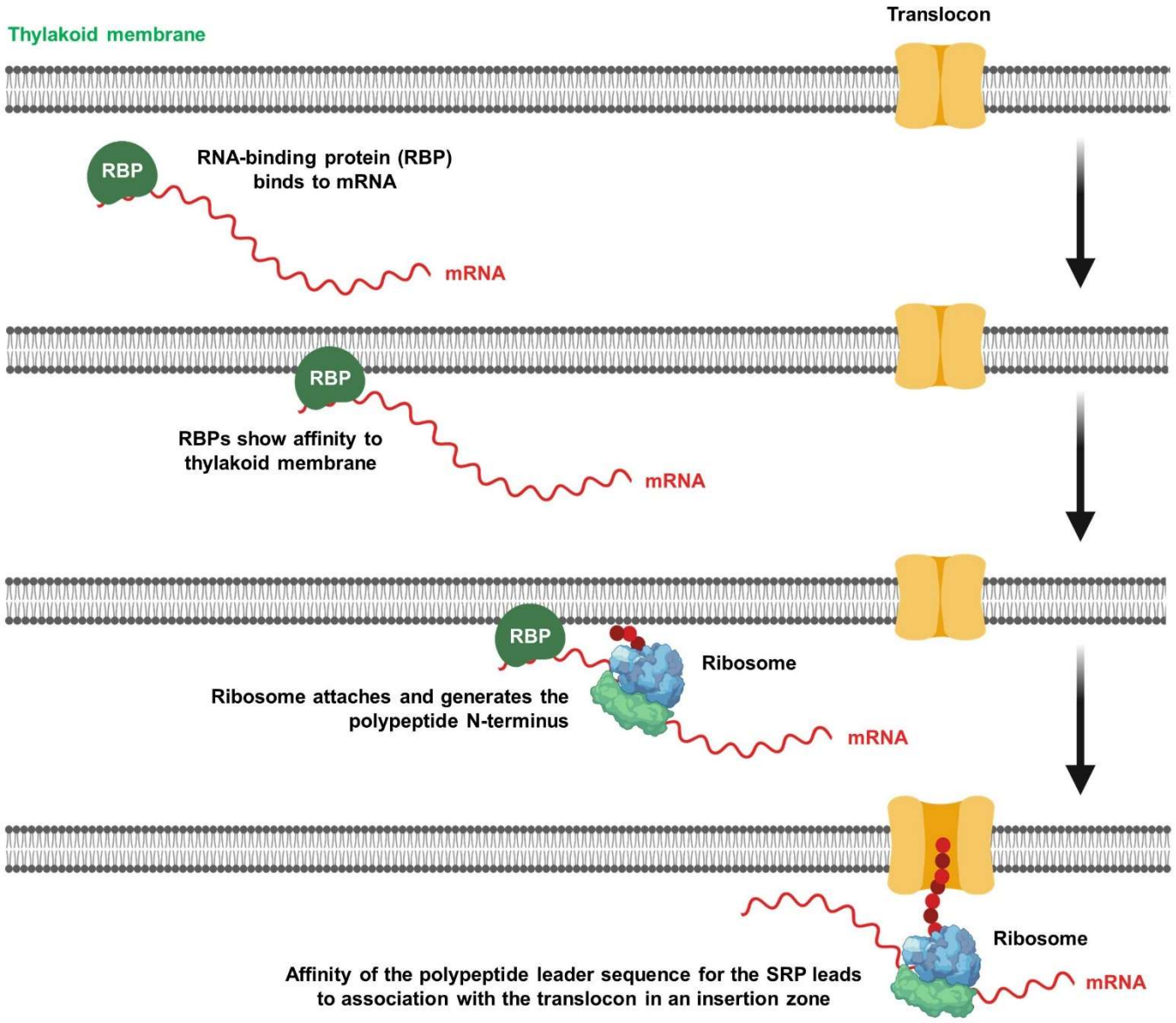

Figure 6: Model for thylakoid membrane targeting based on recognition of thylakoid-mRNA molecules by specific RNA-binding proteins with affinity for the thylakoid membrane surface. Following association with the thylakoid membrane surface, ribosomes bind and initiate translation. Affinity of the N-terminal leader sequence of the nascent polypeptide for the Signal Recognition Particle (SRP) then promotes association with the translocon, which is concentrated in specific zones at the inner surface of the thylakoid system (adjacent to the central cytoplasm) or on thylakoid protrusions into the central cytoplasm in *Synechocystis.* In *Synechococcus*, the initial association with the thylakoid is quite delocalised over the membrane surface (as observed in the presence of puromycin) but active translation leads to concentration at insertion zones. Ribosome binding likely displaces RBPs from the mRNA, leading to a loss of thylakoid association in the presence of lincomycin.

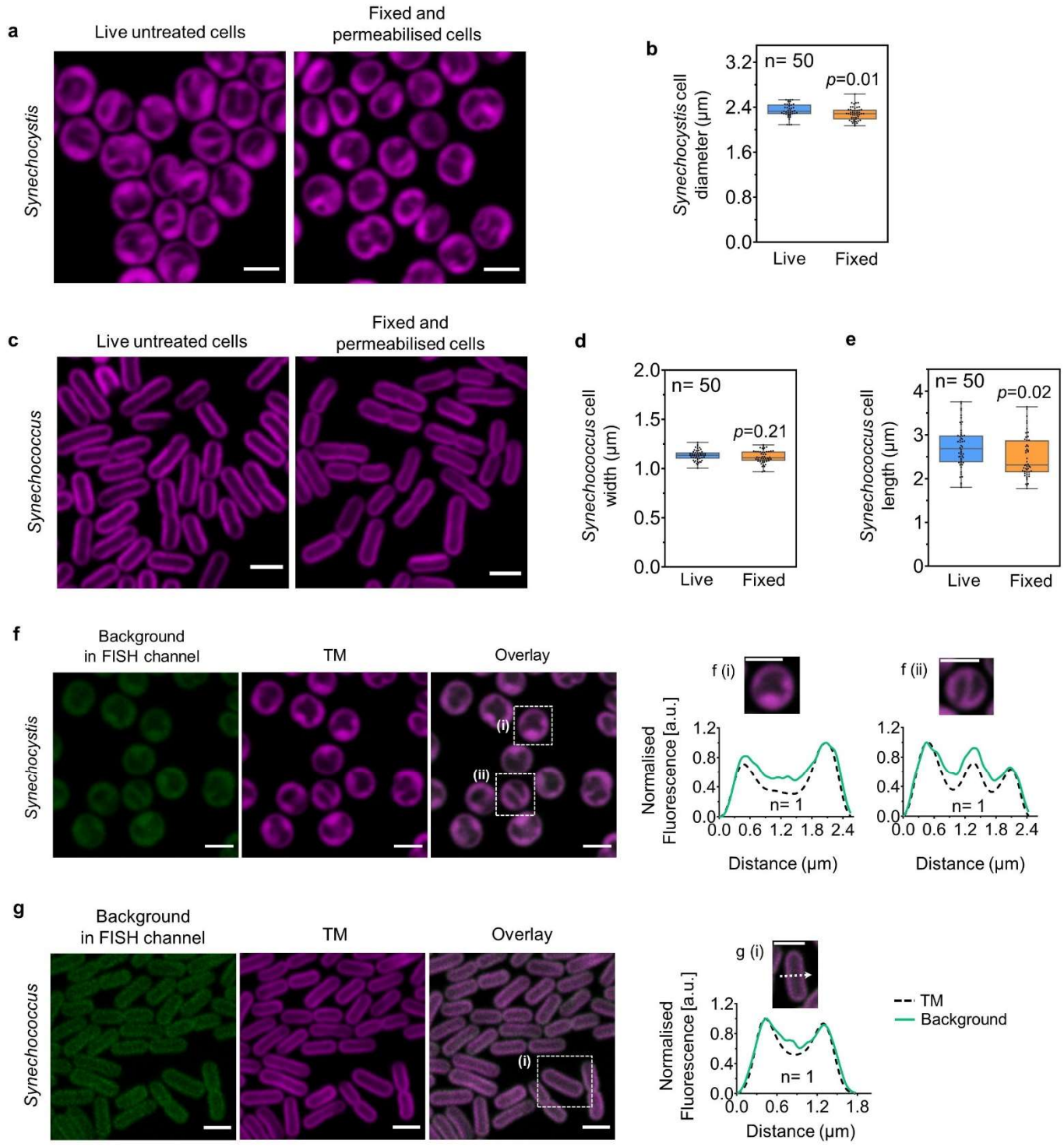

Extended Data Figure 1: **Background fluorescence in fixed cells of *Synechocystis* and *Synechococcus. a,*** Confocal fluorescence images of photosynthetic pigments in *Synechocystis* cells showing thylakoid membrane organisation without and with the fixation and permeabilisation used for mRNA-FISH probing. **b,** statistics for cell diameter in fixed vs live cells (*n* = 50 cells: no adjustments for multiple comparisons). **c,** Confocal fluorescence images of photosynthetic pigments in *Synechococcus* cells showing thylakoid membrane organisation in live vs. fixed cells. **d,e,** statistics for cell width and length in fixed vs live cells (*n* = 50 cells: no adjustments for multiple comparisons). **f,g,** Confocal micrographs of *Synechocystis* **(f)** and *Synechococcus* **(g)** cells (fixed and permeabilised but not probed)

786 showing the background signal (green) in the TAMRA detection channel in comparison to fluorescence from the
787 photosynthetic pigments (TM, in red). Line profiles drawn from representative cells of both *Synechocystis* **(f. i,ii)** and
788 *Synechococcus* **(g, i)** confirm that the background signal (green line) colocalises with the TM (black dashed line).
789 TAMRA channel shown without background correction. Images are representative of at least 2 independent
790 experiments. Error bars in the box plots indicate the range of values recorded, the centre line shows the median and
791 the box spans the interquartile range. *p* values are from unpaired two-tailed Student's t-tests. Scale bars: 2 µm.
792
793

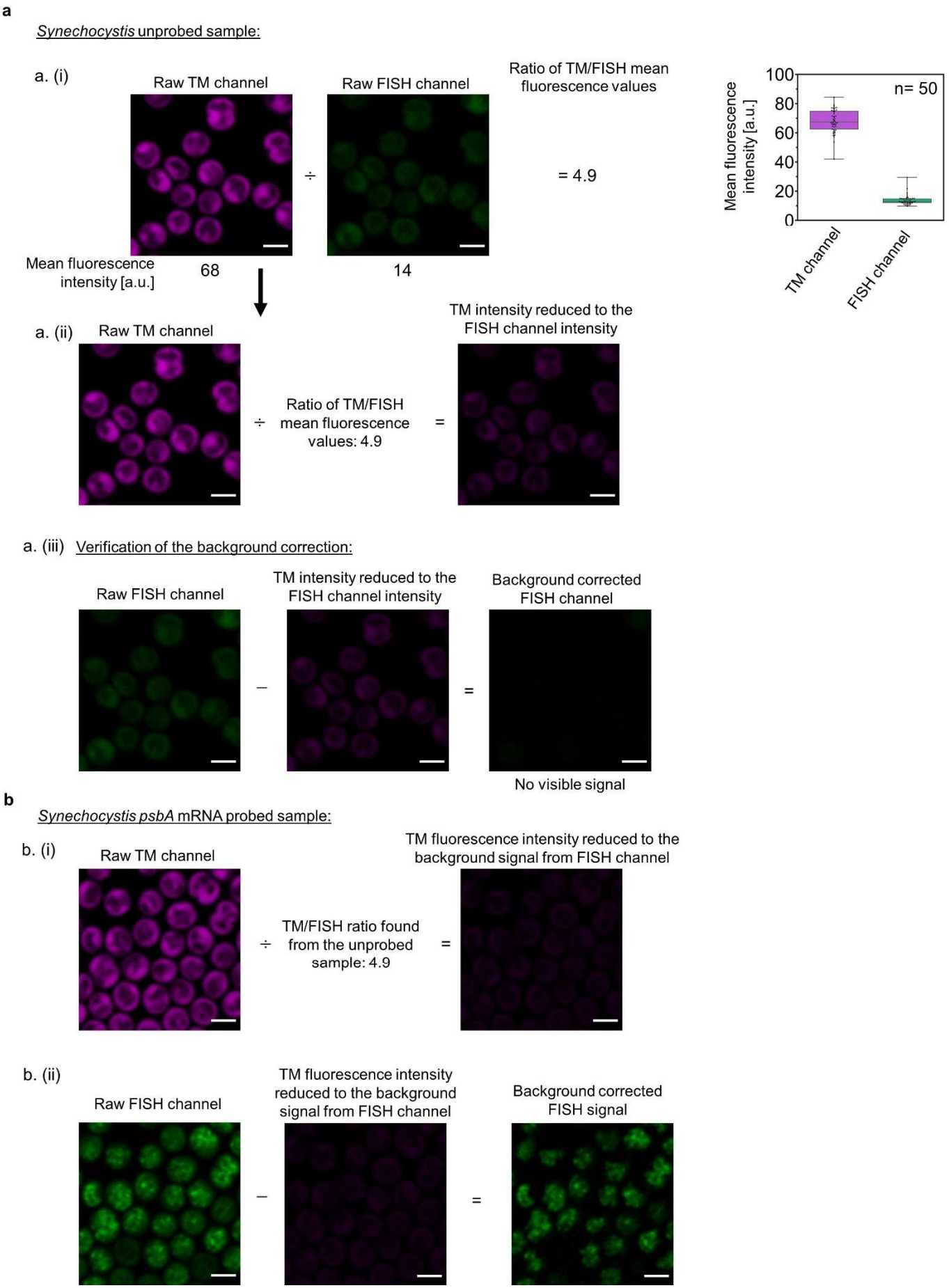

794

795 **Extended Data Figure 2: Correcting for background fluorescence in RNA-FISH micrographs.** Step-by-step illustration

796 of the procedure used to subtract background fluorescence from the FISH images, illustrated with *psbA* mRNA in

Synechocystis as an example. **a,** demonstration that the signal in the TAMRA channel is a predictable fraction of the signal in the TM channel in unprobed cells (*n* = 50 cells); **b,** use of this principle to remove background signal from FISH images in probed cells. Images are representative of at least 2 independent experiments.

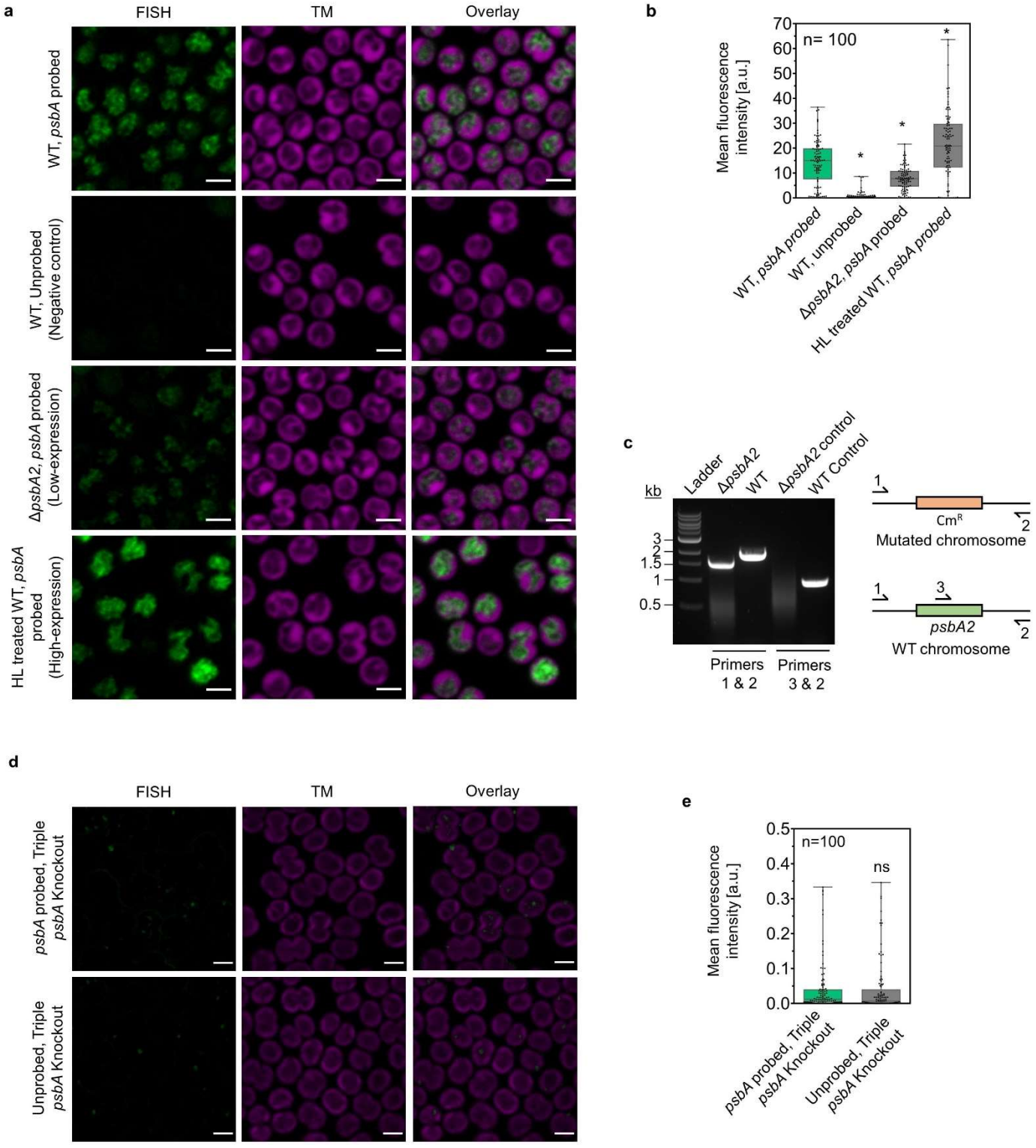

Extended Data Figure 3: Controls for specificity of *psbA* mRNA-labelling in *Synechocystis*. **a**, Variation in *psbA* mRNA signal intensity between WT grown under standard conditions (first row) and three control samples: unprobed, Δ*psbA2* mutant (probed with *psbA2* mRNA probes) and high light (HL: 600 µmol photons $m^{-2}s^{-1}$, 1 hour) - treated cells similarly probed. Micrographs showing the FISH channel (green) vs. TM (magenta). **b,** Mean intensity of the mRNA signal in the different samples. Analysis was done after smoothing the images (below optical resolution) and correcting the background signal in the FISH detection channel (detail in Methods): n = 100 cells; p=4x10^{-27} for

WT probed vs unprobed, $5x10^{-9}$ for Δ*psbA2* vs WT, $4x10^{-5}$ for HL vs normal growth. **c,** Confirmation of full segregation status of Δ*psbA2* mutant by PCR amplification using the primer pair illustrated at the right hand side of the gel image (detail in Methods); **d,** Micrographs showing the triple *psbA* knockout[29] ± *psbA* probe; **e,** Quantification of FISH signal from the triple *psbA* knockout ± *psbA* probe (*n* = 100 cells; *p*= 0.9). Analysis was done after smoothing the images (below optical resolution) and correcting the background signal in the FISH channel (detail in Methods). Images are representative of at least 2 independent experiments. Error bars in the box plots indicate the range of values recorded, the centre line shows the median and the box spans the interquartile range, *n*: number of cells measured, *: significant difference from the untreated cells, at *p*< 0.001, measured by unpaired two-tailed Student's t-test; ns= *p*-value non-significant; scale bars: 2µm.

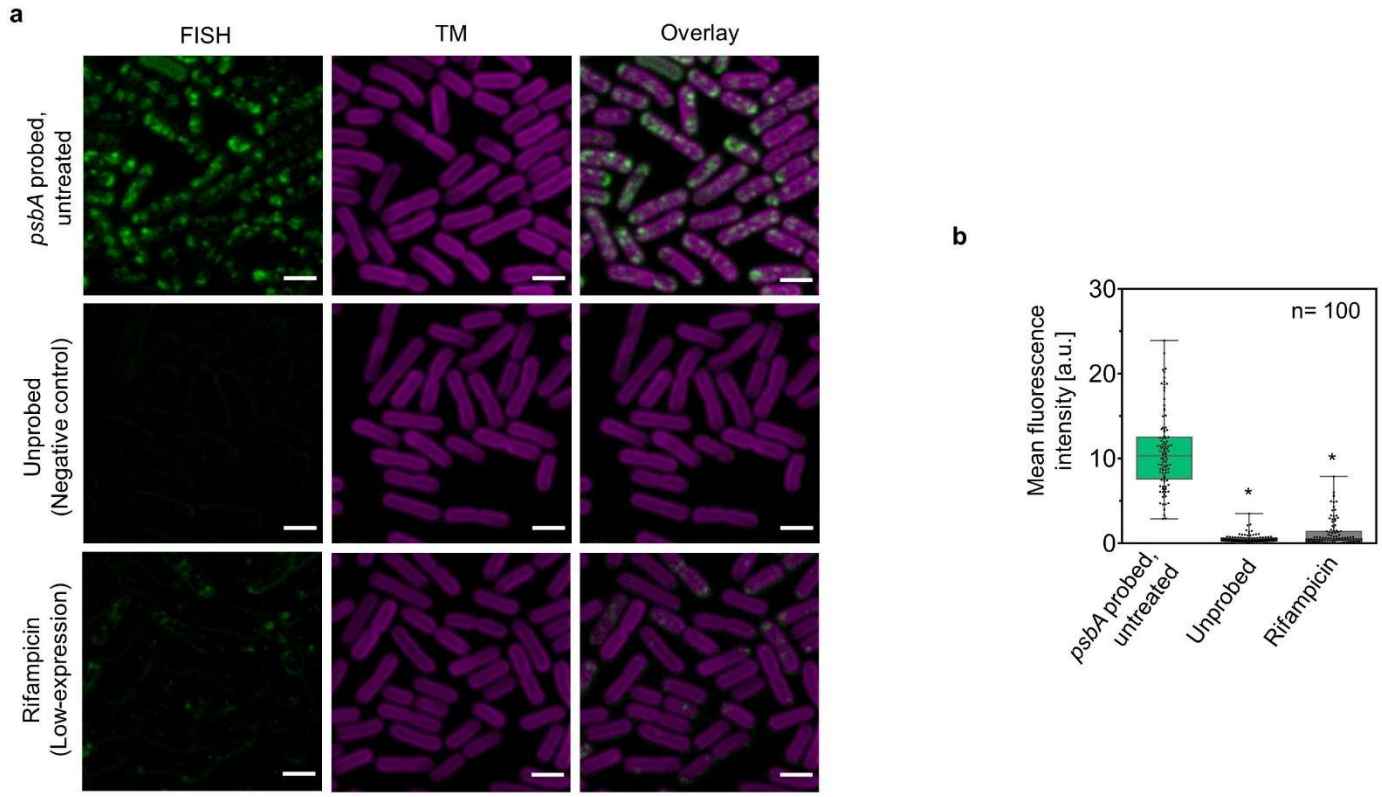

818

819 **Extended Data Figure 4: Controls for specificity of *psbA* mRNA-labelling in *Synechococcus***. **a**, Comparison of *psbA*
820 mRNA signals in cells grown under standard conditions (first row) and unprobed and rifampicin-treated cells.
821 Micrographs of the mRNA FISH signal (green) and TM (magenta). **b,** Mean fluorescence intensity per cell of the
822 mRNA signal in cells from the different samples: $p=6\text{x}10^{-41}$ for probed vs unprobed, $5\text{x}10^{-40}$ for rifampicin vs
823 untreated. Analysis was done after smoothing the images (below optical resolution) and correcting the background
824 signal in the FISH channel (detail in Methods). Error bars in the box plots indicate the range of values recorded, the
825 centre line shows the median and the box spans the interquartile range. Images are representative of at least 2
826 independent experiments. n: number of cells measured, *: significant difference, at $p< 0.001$, measured by unpaired
827 two-tailed Student's t-test; scale bars: 2µm.

828

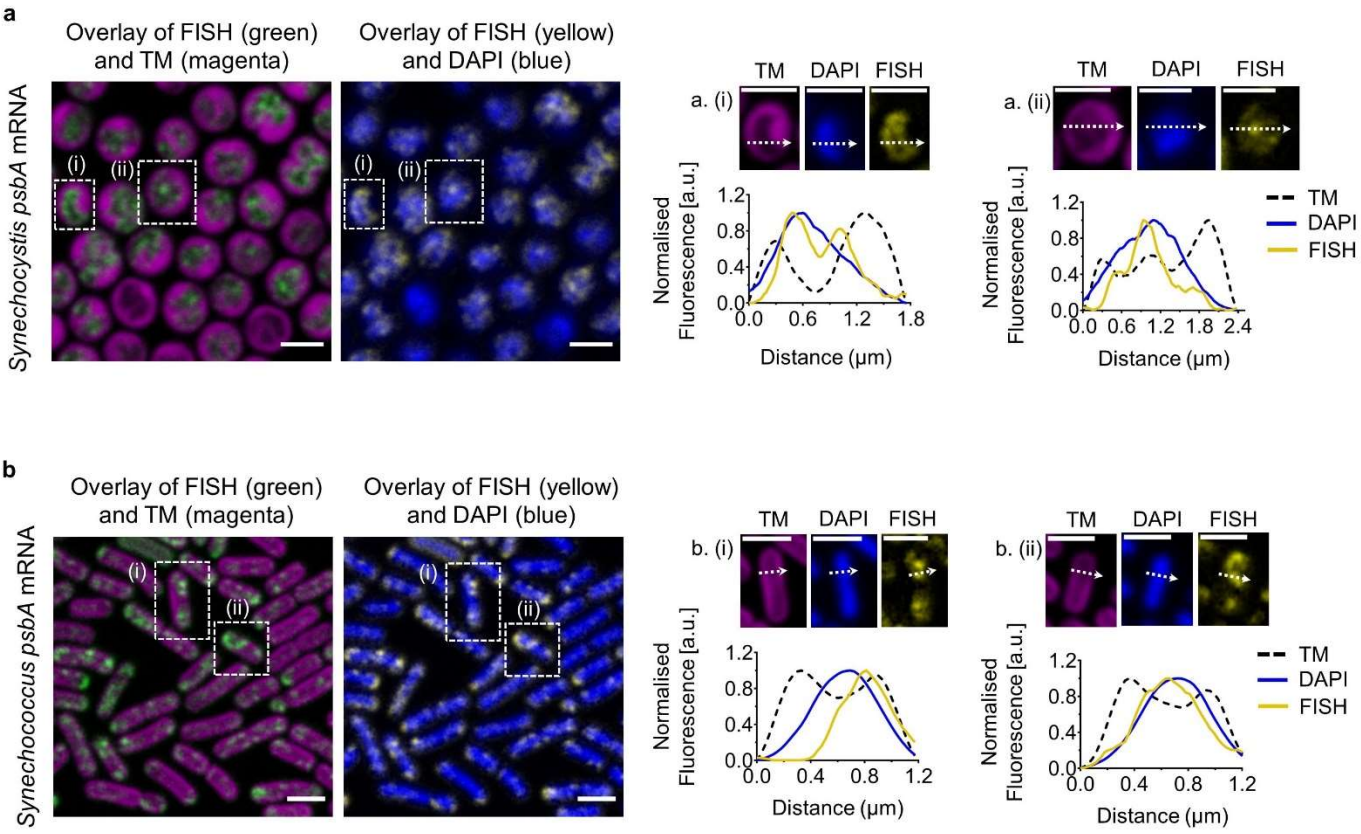

Extended Data Figure 5: Localisation of *psbA* FISH signals relative to thylakoid membrane (TM) and nucleoids (DAPI-stained) in *Synechocystis* and *Synechococcus.* a, *psbA* mRNA in *Synechocystis* relative to TM and DAPI. Line profiles (a, i-ii) across representative cells show the distribution of TM, FISH and DAPI signals in *Synechocystis.* **b,** *psbA* mRNA in *Synechococcus* relative to TM and DAPI. Line profiles (b, i-ii) across the short axis of representative cells show the distribution of TM, FISH and DAPI signals in *Synechocystis.* Images are representative of at least 2 independent experiments. Scale bars: 2μm.

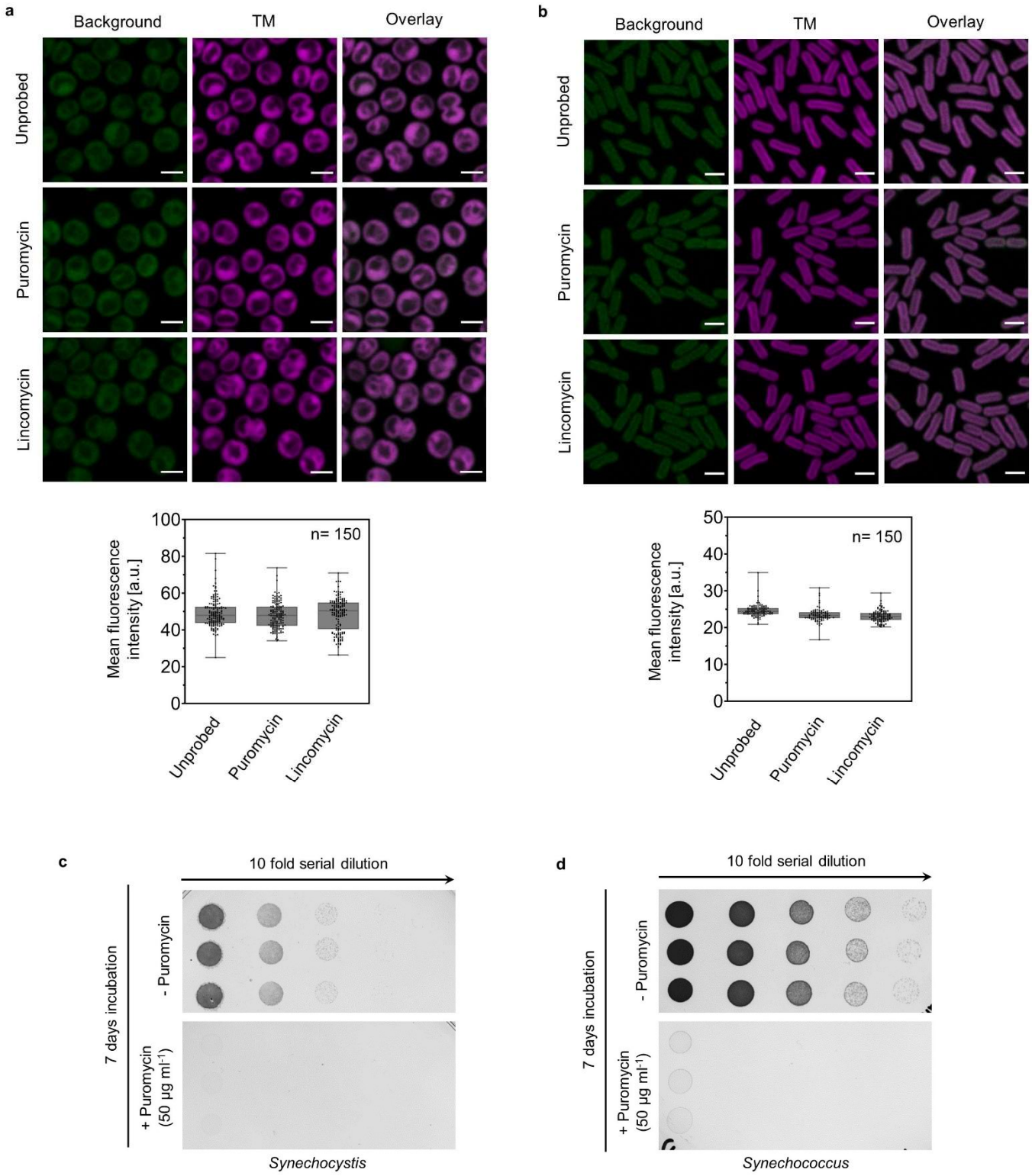

Extended Data Figure 6: Effects of puromycin and lincomycin treatments. a,b, Controls showing that puromycin and lincomycin treatments do not increase background autofluorescence. Confocal fluorescence micrographs and mean fluorescence intensity per cell of the background signal in the TAMRA channel for unprobed cells of (**a**) *Synechocystis* and (**b**) *Synechococcus*, showing similar intensity of the background autofluorescence with and without inhibitor treatment. Error bars in the box plots indicate the range of values recorded, the centre line shows the median and the box spans the first to third quartiles; none of the differences are significant. n: number of cells

844 measured; Scale bars: 2 µm. **c,d,** Effects of puromycin on growth of *Synechococcus* and *Synechocystis* cells. Ten-fold
845 serial dilutions of three independent cultures were spotted on BG11 plates ± puromycin (50 µg/ml). Plates were
846 photographed after seven days of growth. Images are representative of 2 independent experiments.

847

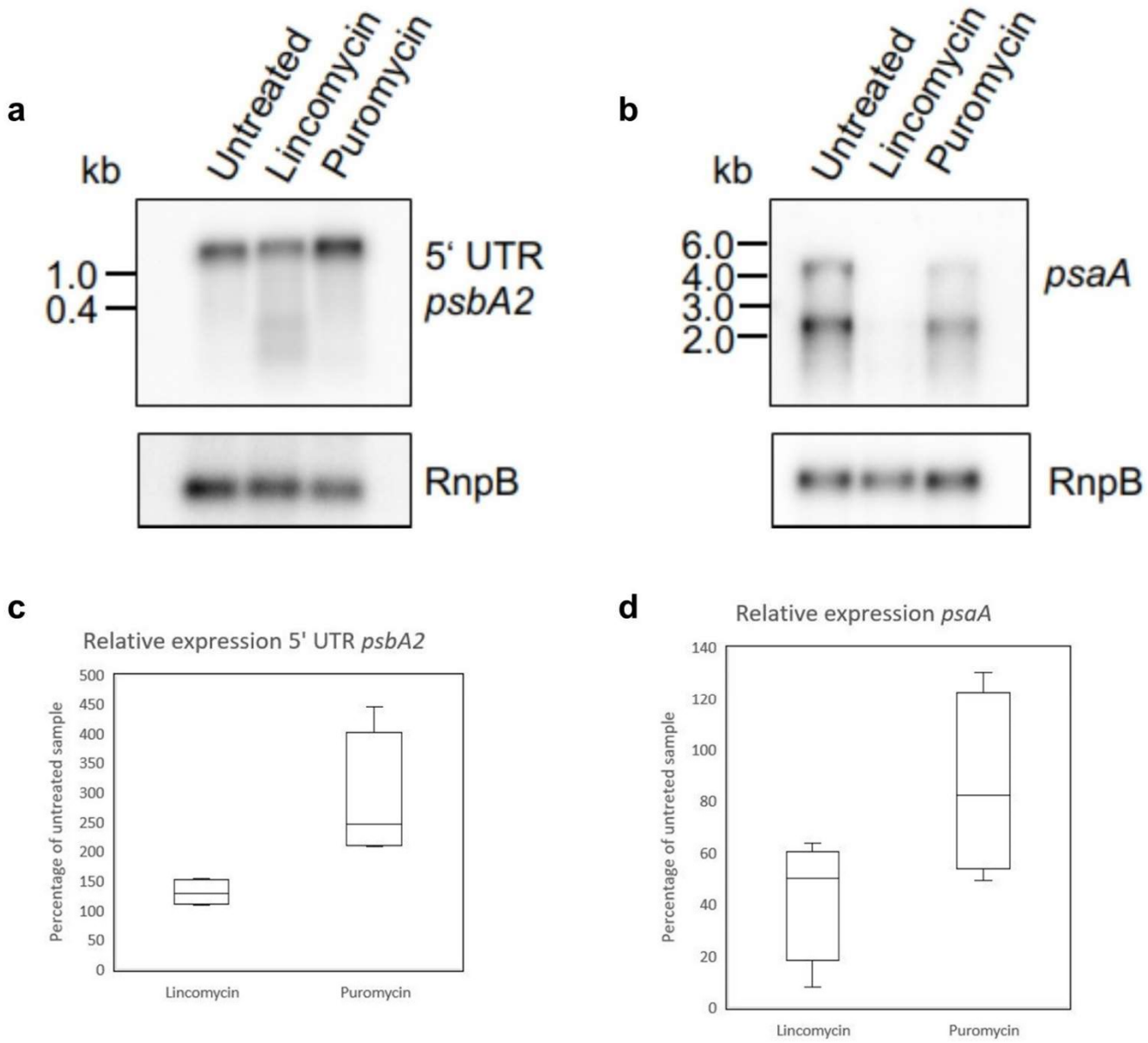

Extended Data Figure 7: Effects of ribosome inhibitors on *psbA2* and *psaA* transcript levels. RNA isolated from *Synechocystis* cells treated with lincomycin or puromycin was separated by electrophoresis, blotted onto a nitrocellulose membrane and hybridized with radioactively labeled probes against the 5’ UTR of *psbA2* mRNA and *psaA*. A probe against the RNA subunit of the ribonuclease P (RnpB) was used as a control. **a,b,** Representative gel images. See Source Data for full-length gel images. Results shown are representative of 2 biological replicates, each with 2 technical replicates. **c,d,** Plots showing *psbA2* (c) and *psaA* (d) mRNA levels (normalised to the RnpB signal) in inhibitor-treated cells relative to untreated cells, combining data from all 4 replicates. Error bars in the box plots indicate the range of values recorded, the centre line shows the median and the box spans the first to third quartiles. The puromycin-treated sample hybridized with *psaA* is not significantly different from the untreated sample (p = 0.245). Other differences are all significant at $p < 0.05$ (p = 0.036 for *psbA2*/lincomycin; 0.021 for *psbA2*/puromycin; 0.009 for *psaA*/lincomycin), measured by unpaired two-tailed Student’s t-tests.

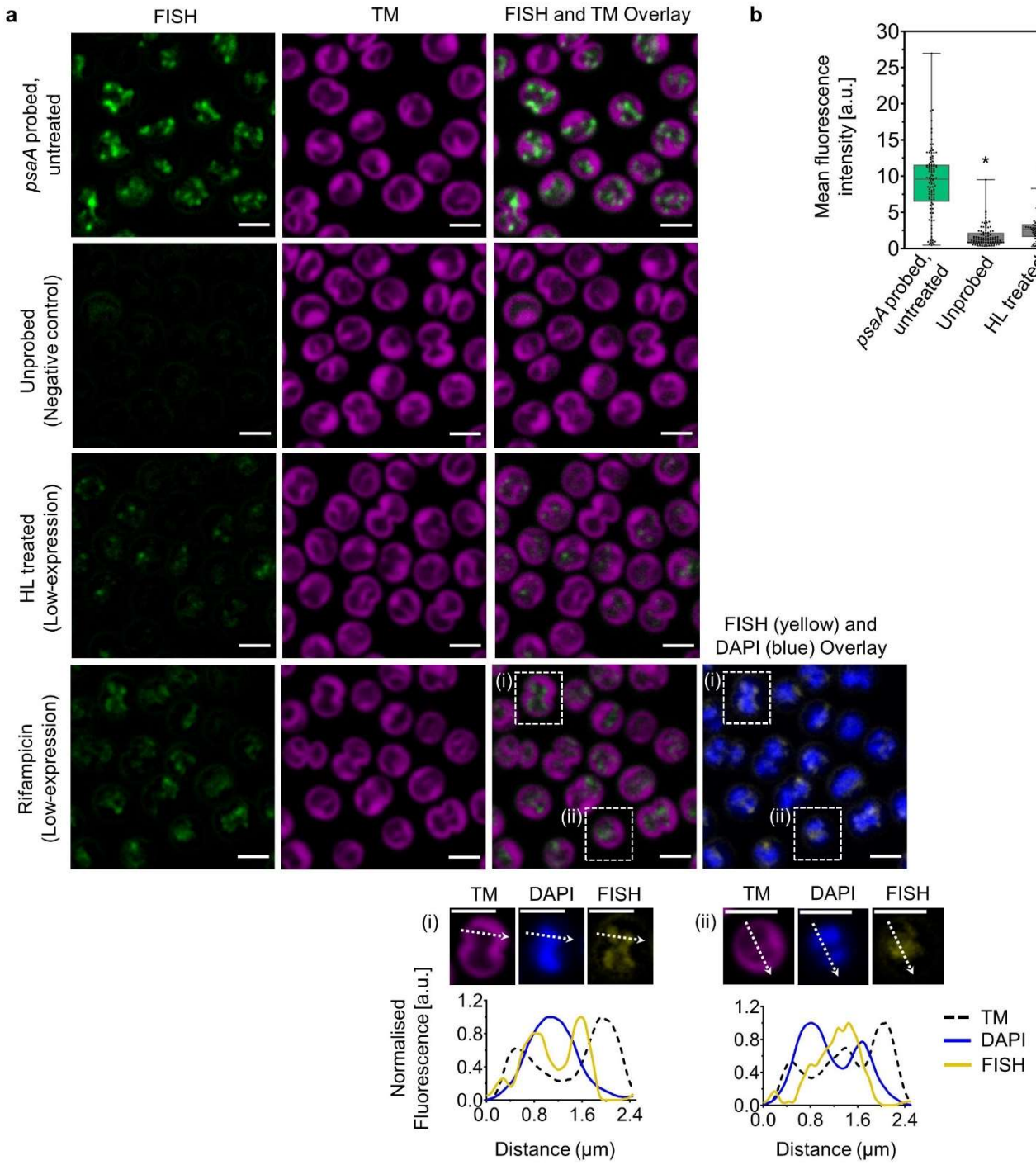

Extended Data Figure 8: Controls for specificity of *psaA* mRNA labelling in *Synechocystis*. **a,** Variation in *psaA* mRNA signal intensity between cells grown under standard conditions (first row) and 3 control samples: unprobed, high light (HL)-treated cells (600 μmol photons $m^{-2}s^{-1}$, 1 hour) and Rifampicin-treated (400 μg ml^{-1}, 1 hour) cells. Confocal fluorescence micrographs showing FISH signal in green and TM in magenta. An overlay between the DAPI-stained nucleoid region (blue) and FISH signal (yellow) is shown for rifampicin-treated cells. Line profiles from representative cells are shown below the corresponding micrographs. **b,** comparison of mRNA FISH signals per cell in the different conditions (p=3x10^{-29} for probed vs unprobed, 8x10^{-25} for HL vs normal growth and 2x10^{-9} for rifampicin vs untreated). Images smoothed (below optical resolution) and corrected for the background signal in the FISH channel.

Error bars in the box plots indicate the range of values recorded, the centre line shows the median and the box spans the first to third quartiles. n: number of cells measured, *: significant difference from the untreated cells, at $p < 0.001$, measured by unpaired two-tailed Student's t-test; scale bars: 2µm.

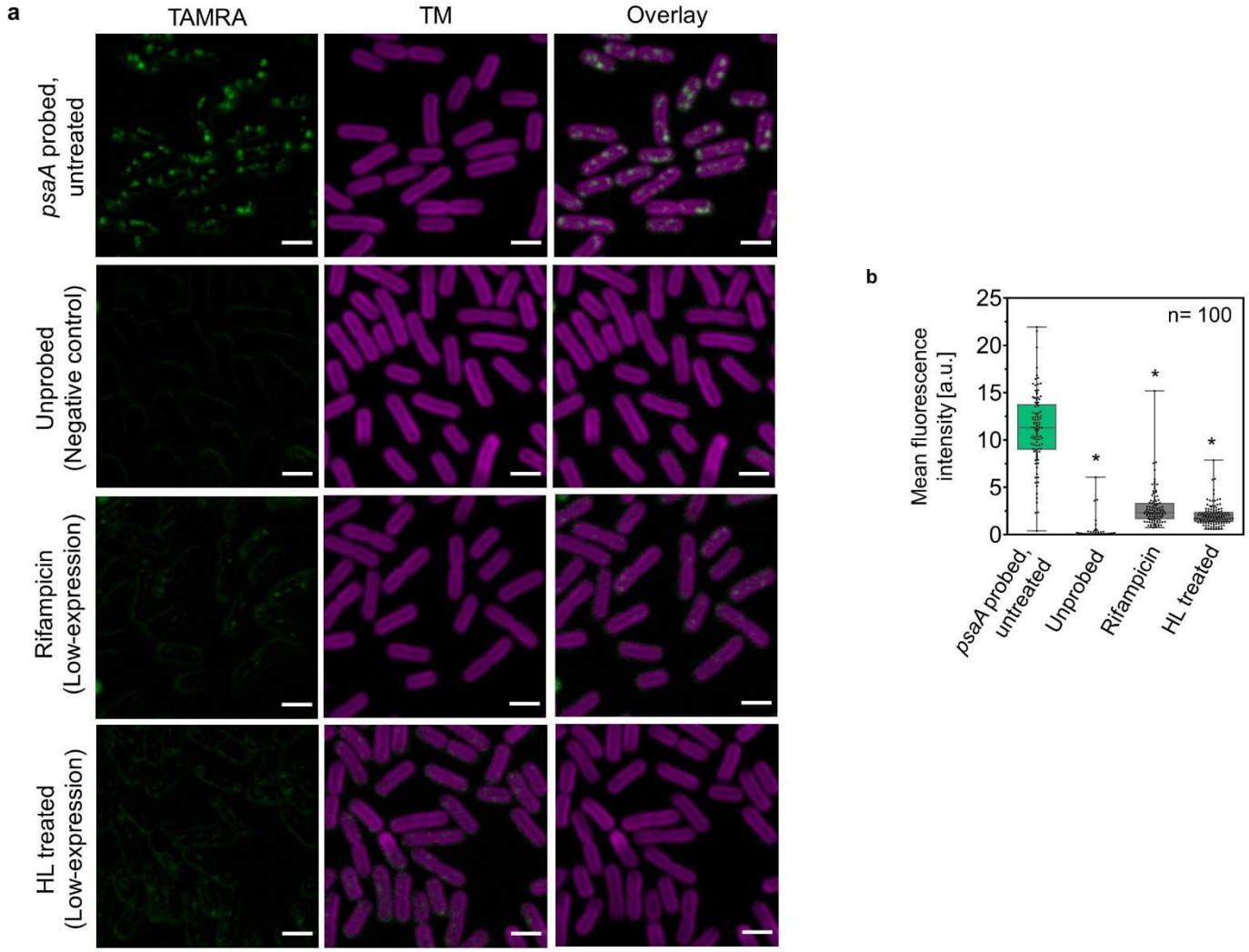

873

874 **Extended data Figure 9: Controls to demonstrate specificity of *psaA* mRNA labelling in *Synechococcus*. a,** Variation
875 in *psaA* mRNA signal intensity between cells grown under standard conditions (first row) and the three control
876 samples: unprobed, Rifampicin-treated (400 µg ml^{-1}, 1 hour) and high light (HL)-treated cells (600 µmol photons $m^{-2}s^{-1}$
877 , 1 hour). Confocal fluorescence micrographs showing FISH signal in green and thylakoid membrane region in
878 magenta. **b,** Comparison of mRNA signal in the control samples compared with the experimental sample. Images
879 smoothed (below optical resolution) and corrected for the background signal in the FISH channel (p=2x10^{-50} for
880 probed vs unprobed; 8x10^{-42} for rifampicin vs untreated; 8x10^{-44} for HL vs normal growth). Error bars in the box plots
881 indicate the range of values recorded, the centre line shows the median and the box spans the interquartile range.
882 Images are representative of at least 2 independent experiments. n: number of cells measured, *: significant
883 difference from the untreated cells, at p< 0.001, measured by unpaired two-tailed Student's t-test; scale bars: 2µm.

884

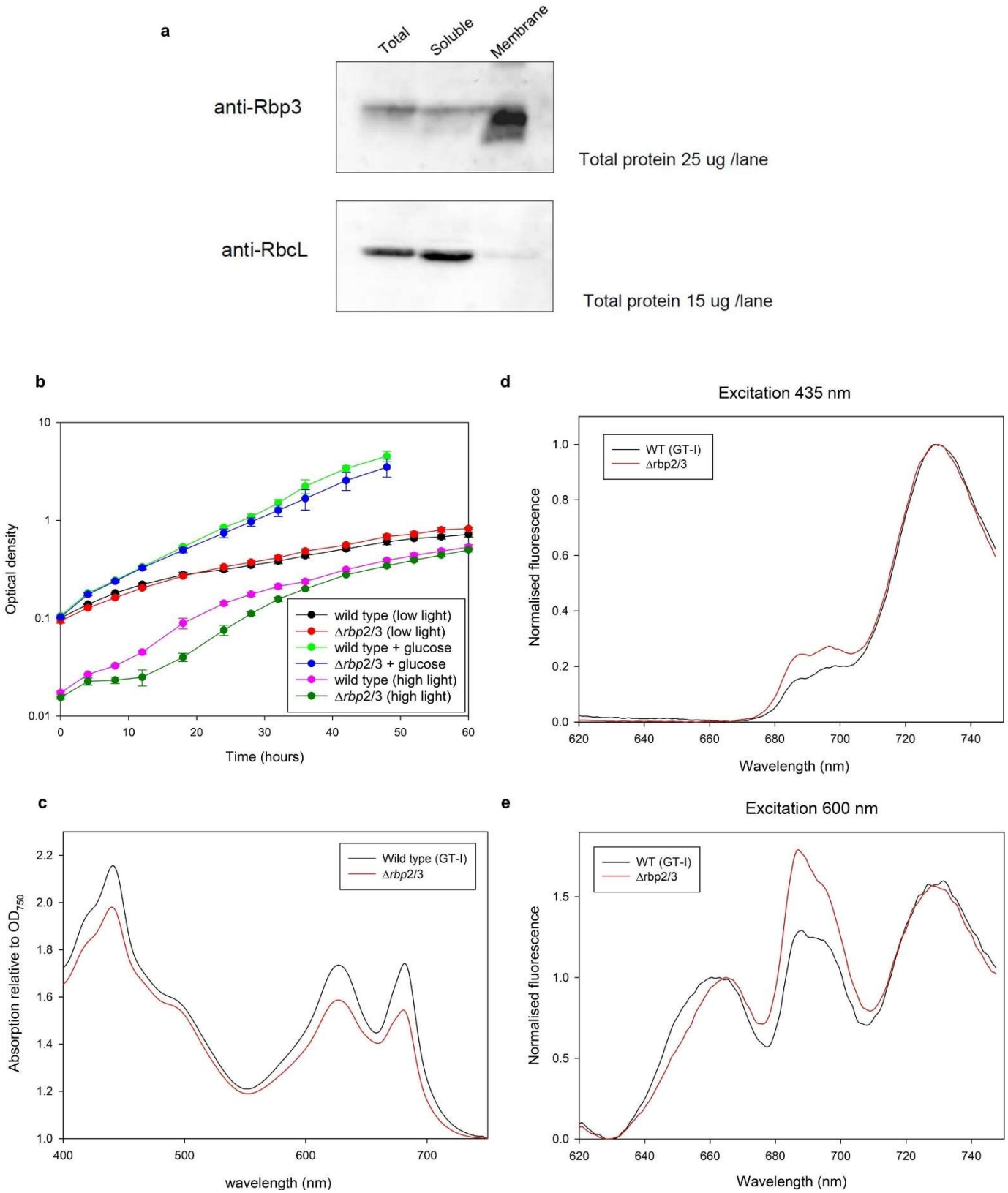

Extended data Figure 10: *Synechocystis* Rbp3 location and photosynthetic phenotype of the Δ*rbp2/3* mutant. a, Western blotting showing that Rbp3 is associated with the membrane fraction. See Source Data for full-length gel images with molecular weight markers. Data shown are representative of 2 biological replicates with similar results. **b,** growth curves for Δ*rbp2/3* vs. the wild-type (GT-I) background in different conditions: 50 µmol photons $m^{-2}s^{-1}$ (low light), 80 µmol photons $m^{-2}s^{-1}$ (high light), or low light in the presence of 10 mM glucose. Error bars

indicate standard deviations from 3 replicate cultures. **c,** absorption spectra of cell suspensions, normalised to turbidity at 750 nm. Δ*rbp2/3* has lower pigment per OD_{750}. **d,** florescence emission spectra at 77K with chlorophyll excitation (435 nm) normalised to PSI emission at 725 nm. **e,** florescence emission spectra at 77K with phycocyanin excitation (600 nm) normalised to phycobilin emission at 660 nm. Δ*rbp2/3* has lower PSI emission (725 nm) relative to PSII (peaks at 685 and 695 nm). All spectra are representative of similar results from 3 independent cultures.

Supplementary Tables

Supplementary Table 1: mRNA-FISH probe sets

a, Oligonucleotide probes designed against *Synechocystis psbA2* (slr1311) gene sequence.

Probe number	Sequence (5' to 3')	Probe number	Sequence (5' to 3')
1	TGTTGGAGAGTCGTTGTCAT	23	TGTGCTCAGCTTGGAACACG
2	AGGTCACCCACTGACAAAAC	24	TGGAAGGGGTGCATCAGGAT
3	ACATAAATCCGGTTGTTGGT	25	TACACCAGCCACACCTAACA
4	GATCATCAAGGTACCGAACC	26	CGGAGAACAAGCTACCACCG
5	AAGTGGTGGCAGTTAAGAGG	27	GTTACCAAGGAACCGTGCAT
6	CGGCGATGAAGGCAATGATG	28	TGGTTTCACGCACCAAGGAG
7	GATACCGTCGATGTCAACGG	29	CGTAGTTCTGGGATTCAACT
8	AGCAAAGAACCAGCAACGGG	30	TTCTTCTTGACCGAATTTGT
9	CCAGAGATGATGTTGTTACC	31	CGGCAACGATGTTGTAGGTT
10	CGATAGCGTTGGAAGAAGGT	32	GATCAACCGACCAAAGTAGC
11	CAGATGGGGTAGAAGTGCAA	33	CGGCTGTTGTTGAAAGAAGC
12	CTCATCTAAGGAAGCGGCTT	34	AAGCACCCAAGAAGAAGTGC
13	TAAGGACCACCGTTGTACAA	35	GAACCAGATGCCGATTACAG
14	GCCGATGAGGAAGTGGAATA	36	CATGGTGCTTACACCCATAG
15	GACGACCCATGTAGCAGAAA	37	GTTGAAACCGTTCAGGTTGA
16	CTAAGCGGTAGGAAAGTTCC	38	CTATCCAAGATGGACTGGTT
17	ACACAAATCCAAGGACGCAT	39	TTGGCTCGGTTCAATACATC
18	GGATACGGGGGCAGAGTAAG	40	ATTGCGTTCGTGCATTACTT
19	GATCAAGAATACGGCGGTGG	41	CTAAGTCGAGGGGGAAGTTG
20	AGAAGGAGCCTTGACCAATG	42	TCAAAGCCACAGGAGCTTGC
21	ATACCCAAGGGCATACCATC	43	TAACCGTTGACAGCAGGAGC
22	CATGAAGTTGAAGGTACCAG		

b, Oligonucleotide probes designed against *Synechococcus psbAI* (Synpcc7942_0424) gene sequence.

Probe number	Sequence (5' to 3')	Probe number	Sequence (5' to 3')
1	TCGCGAAGAATGCTGGTCAT	21	ACATGAAGTTGAAGGTGCCG
2	GATCCCAAACGTTATCGCGG	22	TTGTGCTCTGCTTGGAACAC
3	CTGGTTACCCACTCACAAAA	23	TGTGGAAGGGGTGCATCAAA
4	CGAACCAACCCACGTAGATG	24	AGAACAGCGAACCACCGAAC
5	AGAGTGGGGATCATCAGCAC	25	CACCAACGAACCGTGCATTG
6	ATGAAGCAGATGGTGGCGGT	26	TAGTTTTGGCTCTCGGTCTC
7	AGGGGCTGCAATGAACGCAA	27	CTCTTGACCAAATTTGTAGC
8	ATACATGAGAGAGCCGGCAA	28	CCACGATGTTGTAGGTCTCT
9	CGCCGGAAATGATGTTGTTG	29	ATCAAGCGACCGAAGTAACC
10	GCGTTGCTGGAAGGAACAAC	30	GTTGAACGATGCGTATTGGA
11	GCTTCCCAAATCGGATAGAA	31	GGAAGAAGTGCAGCGAACGG
12	TTGTACAGCCACTCGTCGAG	32	CATGGAGGTAAACCAGATGC
13	CCACTAATTGGTAAGGACCA	33	TGAACGCCATGGTGCTGATG
14	ATACCCAGCAAGAAGTGGAA	34	ACTGGTTGAAGTTGAAACCA
15	ATTGACGACCCATGTAGCAG	35	TTGCCTTGGCTATCCAAAAC
16	ATACCGAGGCGGTACGACAG	36	ATCTGCCCAAGTGTTGATCA

17	ATGCAACACAGATCCAAGGG	37	CCAAGTTGGCACGGTTCAAC
18	AAAAGCAGCCGAGAGTGGAG	38	ATTACGCTCGTGCATCACTT
19	CCGATCGGGTAGATCAGAAA	39	AAGTCGAGCGGGAAGTTGTG
20	CATGCCGTCCGAGAACGAAC	40	ATTGAAGGCGCAGTCAAAGC

903

904 **c, Oligonucleotide probes designed against *Synechocystis psaA* (slr1834) gene sequence.**

Probe number	Sequence (5' to 3')	Probe number	Sequence (5' to 3')
1	TCGGGTGGACTAATTGTCAT	25	ATTGAGCGTGCCAAGAAGTA
2	TTATCAACCGAGACTTTGGC	26	AAGAACCTAACAGGGCGAGG
3	TCTCGAAGGAAGTTGGTACC	27	TGTTGTGCAACGATGATCGT
4	CTAAAGTCCGGTCGAAGTGA	28	GGTGGGTGAACAGGGATAAC
5	ATTCCAAATCCAAGTGGTGG	29	ATCACGCACCATGAAGATGG
6	TCTAAATCGCTGGTCTGACT	30	TTATTAACGTTCTTGGCGGG
7	CCCAAAGTGAGCACTGAAGA	31	ACCCAGTTGAGATGGGAAAT
8	AAAATTTCGCGCCGTGGAAG	32	AGCTATGGAAGCCGAGGAAA
9	CACTGGGTTTAATGTGGGTA	33	GTCGTTGTGGATGTAGAGAC
10	AAGATGCCTTGACCGACAAT	34	AAGATCGGTTGCAGTTGGAT
11	AACAGGCCAGACGTAATCTG	35	GGTAAAAGCGTGGATGTGGT
12	TGATAGCTGTCGGTGAAACC	36	ATATAGAACCCCTTTGAGGA
13	CATAACCAAACCGCCAATGG	37	TATCAGGGACAAGGCGAGAG
14	CAATTTGGGAGCTTTGACGT	38	CACAGGGGAAACGGAAACCG
15	CATCATCGACTCCACATTTT	39	AGACCGAGGAAAACGTGGTC
16	CCCAGCATCCAAAAGTTTAT	40	AAGGGAGTTGTACATCCAGA
17	AAGGGGAATGTCCTTAGGAG	41	CATCGGATTGCATTTTCCAA
18	ATCTTGCTCGGTTCCAAAAT	42	TAGGAGTTGATGACGTTGGC
19	TCAAACCTTGGGCAAAGCTG	43	GGCAAAGACAAAGTGTCCGG
20	AGGAAGTCTGAGTAGACTCC	44	CGTCCACTGAACAGGAACAT
21	GATTCAATCCCCCTTTAAAG	45	CCAGACAATGGACTCGATCA
22	AAATGGTGGTGAGCGGTATC	46	CCACATTCAGTTTGTTGTGA
23	TGATGAACAGGACGGCGATC	47	ACGACCTTGAATGATGCTCA
24	GAGGATCTCTTTCATGCTAT	48	ACAATACCTCCGAGGAGATA

905

906 **d, Oligonucleotide probes designed against *Synechococcus psaA* (Synpcc7942_2049) gene sequence.**

Probe number	Sequence (5' to 3')	Probe number	Sequence (5' to 3')
1	GTCGGAACCGGATTTTTATC	25	CTAGGTTGATCGACAGTTGG
2	CTTACCCCACTTCTCAAAAG	26	ACGATGATGCTGATCGAACC
3	TCCAAATCCAAGTTGTGGTT	27	AAGTACGGATACGGAGGCAT
4	AAATCGTGAGCGTTAGCGTG	28	CAATCCAGATGTGGTGAGTA
5	TCAAGGTCACTGGTATGACT	29	TGAAAATGGCAGCGTGAGCA
6	ACCAAAGTGAGCGCTGAAGA	30	AGGAGGTTGTCGACATTCTT
7	ACCAGATAAAGATCACCGCA	31	GTGTCGTTGTGGATGTAGAG
8	CAGCCGCTGAAATTGGAGAA	32	CGAGAACATGTCTTGGGGAC
9	GAAGATCGGCCAAACGACTT	33	AAGATGGGCTGCAGTTGAAT
10	GATCTGAATGCCATGGAAGC	34	GTGCAAGGGCATGAATGTTT
11	CCGTGACGTAGAGCTGAAAC	35	CAAACACTTGGCTGACCGAA
12	CTTTGTGGTAGTGGAACCAG	36	GAATCGTGAAGGCGTGGATG

13	TCGACGTTTTGGAACCATTC	37	GAACTCCGAGCGTAGAGAAC
14	CAAGTGGTGGTTCAACATCG	38	AAGGTTGGCTTTGTCAGGAA
15	CGACACGTGAATCTGGTGAC	39	GAACAAGCCTAGGAACACGT
16	TTTTGCCGTTGAGAACCAAC	40	TCGACAGGGAGTTGTACATC
17	CGGAATATCAGCCGCAGAAG	41	CCAAACATCGGACTGCATTT
18	TCAGGCTGACATCCAAGAAC	42	TTGAGCAAAGTTGCCATTCG
19	AGCGTGAAGAAGGCTTTCAC	43	GACAAAGTGAGCACCCAAGA
20	ACCTTTGAAGGTCAGGAAGT	44	GCCACTGAACAGGAACATCA
21	GTGACCCGCAACAATGAAGA	45	CAGACGATGGACTCGATCAG
22	CCAAGATTTCTTTGAGGCTG	46	CACTTTGAGCTTGTTGTGAG
23	GTGAAAGGACCTTTGTGAGC	47	AGACCATGTGGTCACAATTC
24	TCTCATAGAGACCTTTGTGG	48	AACCAACTGCAATGATGCGG

907

908 **e, Oligonucleotide probes designed against *Synechocystis cpcAB* (sll1577 and sll1578) gene sequence.**

Probe number	Sequence (5' to 3')	Probe number	Sequence (5' to 3')
1	TGTGATAGTTTCTCTGGTGG	25	CTTCTAGAACGGAAGCGTCG
2	TGTGGTTTGTCTGTGATCTA	26	CAACGTAGGTTTCACGGAGA
3	TTCATCAGGAGCCATAAACC	27	CATTTTTTGAACGCCAGCAG
4	TAACGAAGTCGGGATCGTCT	28	CCATTGGGATCGTTAACGAT
5	TCTCTACAGGTGGGTATAGA	29	GCAACGATAGCACTGCAATC
6	ATCCCACCATTTTGATATTC	30	GTCGAAGTAACCAGCGATTT
7	CTACTTTCCTTTTTGAGCTT	31	ATAACCAGACTAGGCTACGG
8	AAGACTGTTGCCTAGGGAAC	32	CGGGTATGGAACCTGAGTAA
9	GTGCGAACTTTTCTCGTTTT	33	GTCAGCTTTAAGCTGGATTT
10	GTTTCGTTCAGCTTATGTTT	34	TATCTCCCGTTAGAATGTGA
11	TAATGTTGCAGGGGATTCTC	35	GCTTCAGTTAAAGGGGTTTT
12	GTGATGGGACTTATGTCTGT	36	TTGAGAGTCAGCGGTGGAAA
13	TAGGCTTGAATGCTTTTGCA	37	AATTCGGTGCTGCTCAGAAA
14	ATCCAGGGAGAAACACGGAG	38	TGCAAACCAGCATTAGCTTG
15	TTAACTACCCGGGGATTTAT	39	ATTGTCGGTCAGAGCTTTAG
16	GGATAAACTGAGGGAGTCCA	40	GTTATAAACGGCTTGGGCAG
17	ACAACCCGAGTGAATACGTC	41	CAGTAGGTAACGATGCGGAG
18	GAGAACCAGAGAGGTACTCG	42	GCGATCAAGTACTCATCCAA
19	GTAGCGCTCAAAGCATCTAA	43	AAGGTGCGGTTGATTTCATC
20	CGGTGATGCGGTTAACAGAA	44	GAGGTAGGAATTAGCTTCGT
21	CAGCGTTGGAAACGATAGCG	45	TGACTAGCTCAGAGCATTGA
22	TGGATTAATTGGGGCTGTTC	46	CCAGGCCAGCTAGAATTAAA
23	ACGCAAACAAGCAGCCATAC	47	AGTTGTTAACACTTTCCCAC
24	GTAGGTAACATAGCGGAGGA	48	GTTCTCCTAGATAAGTGTCA

909

910 **f, Oligonucleotide probes designed against *Synechococcus rbcL* (Synpcc7942_1426) gene sequence.**

Probe number	Sequence (5' to 3')	Probe number	Sequence (5' to 3')
1	TTATAGCCTGCGGCAGATTG	25	TGCGATTTGTGGATTGCATC
2	TGAGTTTGTAGTCCTTCACC	26	TTTGATTTCACCGGTTTCTG
3	GTGTAATCGGGGGTGTAATA	27	CGGTCACGTTCAGGTAGTGA
4	CAGCAGGTCAGTGTCTTTGG	28	TTTCATCATTTCTTCGCAGG
5	CTGAGGGCTGAAGCGGAAAG	29	AGTTCTTTAGCGAACTCAGC

6	GGTACCGGTCGAAGATTCAG	30	CATGCATGATGATCGGCATG
7	GATCCATGTCGGTCAGCAAG	31	GTGAAACCAGCCGTCAAGAA
8	GCTCGATGTGGTAGCACTTG	32	ATTTTGCCAAGGTGGTGTTG
9	TAGGAGTTCTCTTCGCCTTG	33	ATTGCACGGTGGATGTGCAG
10	CGGGTAAGCGATGAACGCAA	34	TTACGCTGACGGTCGATCAC
11	ACCCTTCTTCAAACAGGTCG	35	AAGACACGGAAGTGAATCCC
12	GAGGTCAGGATGTTGGTGAC	36	GGACAGACGCAAACACTTGG
13	AAGCCAAACACGTTACCGAC	37	CAAGGTCGAAGCTTTGTCGC
14	ACGCAGCGAACGGATAGCTT	38	TTCGCGCATCAAGTCAACAA
15	ACGGGGAAGCGGATGTCTTC	39	CCCAATCTTGGGTGAAGAAG
16	CCTTGGAAGGTTTTGACCAA	40	TGGATACCACCGGAAGCAAC
17	GACTTGGATACCGTGGGGAG	41	ATCACCGAAGATTTCCACCA
18	CGTACTTGTTCAGCAGGTCG	42	CACCGAACTGGAGAACGGAG
19	GTTTTGGTTTGATCGTGCAA	43	CAAGCTTCCAAGGCAACACG
20	GTAGTTTTTCGCCGACAGAC	44	TTCACGGTAGAGGTCGCGAC
21	CAGACATTCGTAGACGGCAC	45	CAGCTTCACGAAGGATGTCG
22	GTCTTTGGTGAAGTCCAGAC	46	ACTTGATCTCTTTCCAGAGG
23	GCTGCGAGTTGATGTTTTCG	47	CTTGTCCATCGTTTCGAATT
24	CCACAAACAGGAAGCGATCG		

911

912 **Supplementary Table 2: Oligonucleotide primers used to generate Δ*psbA2* mutant of *Synechocystis***

Purpose		**Sequence (5' to 3')**
Amplification of *psbA2* (slr1311) upstream sequence	Forward primer:	TAGCGTTCCAGTGGATATTTGCTGG
	Reverse primer:	GGGCGTAACGATGTTCAGATTGGAACTG
Amplification of *psbA2* (slr1311) downstream sequence	Forward primer:	ACGTGCCGATCATTCCTTGGTGTAATGCCAAC
	Reverse primer:	ATTCAATCGCTCTAGGCGATCG
Amplification of CmR	Forward primer:	CAGTTCCAATCTGAACATCGTTACGCCCCGCCCTGCCAC
	Reverse primer:	TGGCATTACACCAAGGAATGATCGGCACGTAAGAGGTTC
Amplification of pGEM-T Easy	Forward primer:	CGATCGCCTAGAGCGATTGAATAGCTTGAGTATTCTATAGTGTC
	Reverse primer:	CCAGCAAATATCCACTGGAACGCTAAATTCGCCCTATAGTGAGTCG
psbA2 (slr1311) specific sequence to check segregation status of the mutant	Forward primer:	TGTTCCAAGCTGAGCACAAC

913

914

Supplementary Table 3: Oligonucleotide primers used to construct the Δ*rbp*2/3 mutant and *rbp*3 expression vector.

Purpose		**Sequence (5' to 3')**	**PCR template**
Amplification of *rbp2* (ssr1480) upstream sequence	Forward primer:	CCGGCCACCCCGATTAAATGTG	Genomic DNA of *Synechocystis* GT-I
	Reverse primer:	GATTTATTTATTCTAAATTAGCTCCAAAACCAGAGAA	
Amplification of *rbp2* (ssr1480) downstream sequence	Forward primer:	GGGCGGGGCGTAAGTTTTTGCCTAATTACCTGAATTTAAG	Genomic DNA of *Synechocystis* GT-I
	Reverse primer:	TGGTGGCTCCTAATTCCCGCAGTT	
Amplification of CmR	Forward primer:	TTTTGGAGCTAATTTAGAATAAATAAATCCTGGTGTC	Chloramphenicol resistant gene in pUC303[58]
	Reverse primer:	AATTAGGCAAAAACTTACGCCCCGCCCTGCCACTC	
Fusion of DNA fragments (*rbp2* KO) and check segregation status of the mutant	Forward primer:	CCGGCCACCCCGATTAAATGTG	Mixture of three DNA fragments or genomic DNA of *rbp2* mutant
	Reverse primer:	TGGTGGCTCCTAATTCCCGCAGTT	
Amplification of *rbp3* (slr0193) KO DNA fragment and check segregation status of the mutant	Forward primer:	ACCTCACTGCGTATGACTTCC	Genomic DNA of *rbp3* mutant provided from Prof. Masahiko Ikeuchi
	Reverse primer:	CACCAATTTGCCACTGTCTACC	
Construction of *rbp3* expression vector	Forward primer:	CATCATCATGAATTCATGTCCATTCGTCTCTACG	Genomic DNA of *Synechocystis* GT-I
	Reverse primer:	GTGGTGGTGCTCGAGCTACTGGGCCGCTGTCAGTT	

Supplementary Table 4: Primers used for construction of inducible FLAG-tagged *rbp2* and *rbp3* mutants

Oligonucleotide name	Sequence (3' → 5')	Description
HindIII-ssr1480_fwd	AAGCTTTAGGGTCAGTTGACCGG	Amplification of *ssr1480* (*rbp2*) and introducing Hind III and XhoI restriction sites
XhoI-ssr1480_rev	CTCGAGTCCCCCAGTCTATCAGC	
HindIII-slr0193_fwd	AAGCTTATGCTTATTCCCGTTTGATTG	Amplification of *slr0193* (*rbp3*) and introducing Hind III and XhoI sites
XhoI-slr0193_rev	CTCGAGGTTTTTTATTAAACTCTAAACAGGACAAAG	
pJet-sll0517-Toop_fwd	CGCCGGGCGTTTTTTATTCTCGAGATCTTTCTAGAAGATCTCCTAC AATATTC	Introduction of the ooP-Terminator into the pJet1.2::sll0517 constructs by inverse PCR
pJet-sll0517-Toop_rev	GCAACCGAGCGAACAGGATTTAGCCCGATTTCCCCACCAGAAATA CGGGTAG	
pJet-sll0517-3xFLAG_fwd	TATTGATTATAAAGATGATGATGATAAATAGGGCTTAGTTTTTGTTCG TCGGTTAGTGAAACTTTTTTG	Introduction of a 3x FLAG-Tag into the pJet1.2::sll0517-Toop construct by inverse PCR
pJet-sll0517-3xFLAG_rev	TCATGATCTTTATAATCGCCATCATGATCTTTATAATCCATGTAGCGG CTACCACCATAGCTTTTAC	
pJet-ssr1480-Toop_ fwd	CGGGCGTTTTTTATTCTCGAGATCTTGCTGAAAAACTCGAGCC	Introduction of the oop terminator into the pJet1.2::ssr1480 construct by inverse PCR
pJet-ssr1480-Toop_rev	GCGGCAACCGAGCGAATCCCCCAGTCTATCAGGCAAGCCTGCC TAGCAAA	
pJet-ssr1480-3xFLAG_fwd	TGATATTGATTATAAAGATGATGATGATAAATAAGTTTTTGGCCTAAT TACCTGAATTTAAGATTTCATTC	Introduction of a 3x FLAG tag into the pJet1.2::ssr1480-Toop construct by inverse PCR
pJet-ssr1480-3xFLAG _rev	TGATCTTTATAATCGCCATCATGATCTTTATAATCCATACGAGGGGTT CTCGGTCTTGC	
pJet-slr0193-Toop_fwd	CGGGCGTTTTTTATTCTCGAGATCTTTCTAGAAGATCTCC TACAATATT	Introduction of the ooP terminator into the pJet1.2::slr0193 construct by inverse PCR
pJet-slr0193-Toop_rev	GCGGCAACCGAGCGAAGTTTTTTATTAAAACTCTAAACAGGACAAAG	
pJet-slr0193-3xFLAG_fwd	ATATTGATTATAAAGATGATGATGATAAATAGGTCCACAGGTTTTCCC TGAACCGGAACTGTTC	Introduction of a 3x FLAG tag into the pJet1.2::slr0193-Toop construct by inverse PCR
pJet-slr0193-3xFLAG _rev	CATGATCTTTATAATCGCCATCATGATCTTTATAATCCATCTGGGCCG CTGTCAGTTTTTCTTTTAG	
PpetE-pjet-sll0517 fwd	ATGTCAATTTATGTAGGCAACCTGTC	Amplification of the pJet1.2::sll0517 construct for inserting the PpetE via Aqua-cloning
PpetE-pjet-sll0517 rev	AAGCTTATCTTGCTGAAAAACTCGAG	
pjet-sll0517-PpetE fwd	TCGAGTTTTTCAGCAAGATAAGCTTCTGGGCCTACTGGGCTATTC	Amplification of the *petE* promoter and introducing sequences homologous to pJet1.2::sll0517 constructs up- and downstream
pjet-sll0517-PpetE rev	TTGCCTACATAAATTGACATACTTCTTGGCGATTGTATCTATAGG	
PpetE-pjet-ssr1480 fwd	ATGTCCATTTATGTCGGG	Amplification of the pJet1.2::*ssr1480* constructs for inserting PpetE via Aqua-cloning
PpetE-pjet-ssr1480 rev	AAGCTTATCTTTCTAGAAGATCTC	
pjet-ssr1480-PpetE fwd	CGTATCACGAGGCCAAGCTTCTGGGCCTACTGGGCTATTC	Amplification of the *petE* promoter and introducing sequences homologous to pJet1.2::*ssr1480*
pjet-ssr1480-PpetE rev	TTCCCGACATAAATGGACATACTTCTTGGCGATTGTATCTATAGG	

		constructs up- and downstream.
PpetE-pjet-slr0193 fwd	ATGTCCATTCGTCTCTACGTCGGTAACC	Amplification of the pJet1.2::*slr0193* construct for inserting PpetE via Aqua-cloning
PpetE-pjet-slr0193 rev	AAGCTTATCTTGCTGAAAAACTCGAGCCATC	
pjet-slr0193-PpetE fwd	TCGAGTTTTTCAGCAAGATAAGCTTCTGGGCCTACTGGGCTATTC	Amplification of the *petE* promoter and introducing sequences homologous to pJet1.2::*slr0193* up- and downstream
pjet-slr0193-PpetE rev	ACGTAGAGACGAATGGACATACTTCTTGGCGATTGTATCTATAGG	
pVZ322-hindIII-seq_fwd	TACAACCTATTAATTTCCCCTC	Colony PCR and sequencing of the pVZ322 plasmid and its derivatives
pVZ322-xhoI-seq_rev	ATGAACAATAAAACTGTCTGCT	

921

922

Supplementary Table 5: Primers used for RT-qPCR

Oligonucleotide name	Sequence (3' → 5')	Description
psbA2_qPCR fw	GTTCCAATCTGAACATCGACAAATAC	Primer for *psbA2* amplification for RT/qPCR from fished RNA
psbA2_qPCR rev	CACTGACAAAACTGTTCCCAC	
RnpB_qPCR fw	GCACCAATTTCCCAAGACTAC	Primer for *RnpB* amplification for RT/qPCR from fished RNA
RnpB_qPCR rev	TCTCTTTTTCTAGTGTGCCATTG	
psaA_2TSS_qPCR fw	GTGATGTTTGCTGAAAACGCC	Primer for the amplification of the second TSS of the *psaA* mRNA for RT/qPCR from fished RNA
psaA_2TSS_qPCR rev	GCAGAATAGTGTAATAGAGGAAG	
psaA_qPCR fw	ATAGGAAACCCTTAATAGTTCATTG	Primer for *psaA* amplification for RT/qPCR from fished RNA
psaA_qPCR rev	GTTGTTATCAACCGAGACTTTG	

Supplementary Table 6: Primers used for Northern Blot analysis

Name	Sequence (5' to 3')
*psbA2*_T7	TAATACGACTCACTATAGGGAGCGCGCTGTTGGAGAGTCGTTGTC
*psbA2*_R	AGTCAGTTCCAATCTGAACATCGAC
*psaA*_F	TGGTTCCACTACCACGTCAA
*psaA*_R	ACCATGAAGTCGGCAGTACC
rnpB_F	GAGTTAGGGAGGGAGTTGCGG
rnpB_T7	TAATACGACTCACTATAGGGGCACTGTCCTCACGCTCGC